Chem Soc Rev

REVIEW ARTICLE

View Article Online
View Journal | View Issue

Cite this: *Chem. Soc. Rev.*, 2022, **51**, 6738

C–H bond activation and sequential addition to two different coupling partners: a versatile approach to molecular complexity

Daniel S. Brandes and Jonathan A. Ellman *

Sequential multicomponent C–H bond addition is a powerful approach for the rapid, modular generation of molecular complexity in a single reaction. In this approach, C–H bonds are typically added across π-bonds or π-bond isosteres, followed by subsequent coupling to another type of functionality, thereby forming two σ-bonds in a single reaction sequence. Many sequential C–H bond addition reactions have been developed to date, including additions across both conjugated and isolated π-systems followed by coupling with reactants such as carbonyl compounds, cyanating reagents, aminating reagents, halogenating reagents, oxygenating reagents, and alkylating reagents. These atom-economical reactions transform ubiquitous C–H bonds under mild conditions to more complex structures with a high level of regiochemical and stereochemical control. Surprising connectivities and diverse mechanisms have been elucidated in the development of these reactions. Given the large number of possible combinations of coupling partners, there are enormous opportunities for the discovery of new sequential C–H bond addition reactions.

Received 31st May 2022

DOI: 10.1039/d2cs00012a

rsc.li/chem-soc-rev

1. Introduction

C–H functionalization has gained significant attention and achieved widespread application as a versatile synthetic approach utilising simple chemical inputs (Scheme 1(a)).[1–10] This strategy enables the efficient coupling of ubiquitous C–H bonds with a large variety of different functional groups under transition metal catalysed conditions, often with high atom-economy. C–H functionalization generally employs mild conditions without the need for strongly acidic or basic conditions, thus rendering it highly functional group compatible. Numerous catalyst systems have been developed for application to C–H functionalization, including both precious metals and their earth abundant first row congeners.

Department of Chemistry, Yale University, 225 Prospect St., New Haven, Connecticut 06520, USA. E-mail: jonathan.ellman@yale.edu

Daniel S. Brandes

Daniel S. Brandes obtained his BA degree in Chemistry from Williams College in 2018, where he worked under the supervision of Professor Jimmy Blair on the synthesis of broad-spectrum antibiotics. He is currently a PhD student with Professor Jonathan Ellman at Yale University, where he is focused on the development of new sequential, multicomponent C–H bond addition reactions.

Jonathan A. Ellman

Jonathan A. Ellman is the Eugene Higgins Professor of Chemistry and Professor of Pharmacology at Yale University. He received his BS degree from MIT and his PhD degree from Harvard University under the direction of David Evans. He carried out postdoctoral research with Peter Schultz at the University of California at Berkeley. Prior to moving to Yale in 2010, he was a member of the faculty at UC Berkeley where he held the rank of Professor of Chemistry from 1999 to 2010 and concurrently was appointed as an affiliated Professor of Cellular and Molecular Biology at UC San Francisco.

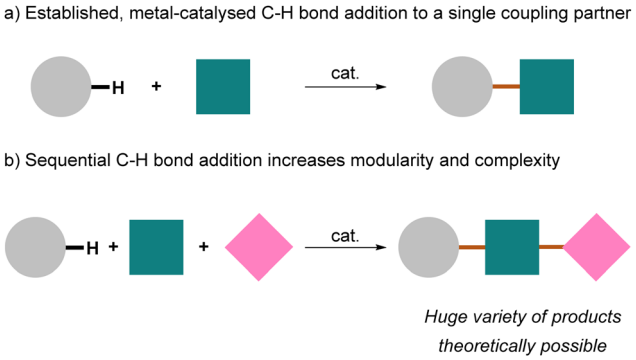

Scheme 1 General depiction of C–H bond addition to one or two coupling partners.

While two-component C–H functionalization continues to be an exciting area of research, the sequential addition of C–H bonds to two different coupling partners has recently emerged as a powerful approach for the rapid and modular generation of molecular complexity. In this new type of transformation, after C–H bond activation and addition to a coupling partner, the reaction is extended by addition to a second, different coupling partner (Scheme 1(b)). In this approach, the metallacycle formed upon initial reaction with the first coupling partner is intercepted by reaction with the second coupling partner, before termination by typical processes like reductive elimination or protodemetalation can occur. Many sequential C–H bond addition reactions involve the insertion of a suitable π-bond or π-bond isostere followed by addition of a different π-bond system such as a carbonyl compound, followed by protodemetalation. Others proceed by oxidative coupling of the second coupling partner to complete the catalytic cycle. These reactions are typically achieved with Cp*M(III) group IX metals, although additional examples employing other catalyst systems have been reported.

The sequential addition of a second coupling partner greatly increases the molecular complexity of the products that are obtained and often enables the generation of multiple stereocentres. Furthermore, these reactions enable the straightforward subdivision of complex structures into simpler and often readily available precursors. The addition of a second coupling partner to these reactions also expands the chemical space combinatorially, thereby affording enormous opportunities for new reaction discovery.

Sequential C–H bond functionalization reactions have inherent challenges that must be overcome for their successful development. For example, after C–H bond activation, selective addition to the first rather than the second coupling partner must occur. Then, after initial selective coupling to the first partner, the reaction sequence must then proceed by selective addition to the second coupling partner rather than adding again to the first partner.[11,12] Moreover, competitive release of a two-component product by protonolysis or oxidation after addition of the first partner must not outcompete the addition of the second partner.

Despite these challenges, sequential C–H bond addition to two different coupling partners represents an exciting advance in transition metal catalysis and provides an efficient, mild, and functional group-compatible approach for the generation of molecular complexity. This approach has already been reported for many different combinations of coupling partners, though the vast majority of possible combinations have not yet been explored. Moreover, through synergistic C–H bond additions, two coupling partners have been utilised even when neither is capable of efficiently coupling on its own.

Unexpected reactivity and bond connectivity have often been discovered during the development of sequential C–H bond addition reactions. Indeed, the diversity of mechanisms that have been elucidated for these transformations is one of the most fascinating aspects of this research.

This review article is organised with respect to the first coupling partner employed in these cascade transformations, which typically contains π-systems or related isosteres. Sections are organised by whether these π-systems are in conjugation or are isolated, and sub-sections delineate the exact classes of π-bond containing coupling partners. In discussions of these different sequential, C–H bond addition reactions, we examine the rationale behind specific choices of coupling partners and the various possible combinations thereof. Reaction mechanisms are also useful to explain the high regio- and stereoselectivities that are often observed for this chemistry, as well as the unexpected bond connectivities obtained for certain reactant combinations. We also comment on the synthetic utility of the complex structures that have been accessed *via* these single step transformations from simple precursors.

2. Sequential C–H bond addition reactions employing conjugated π-systems as the first coupling partner

2.1. Enones as coupling partners

The first sequential C–H functionalization reaction was reported by Ellman and Boerth in 2016 upon exploration of Cp*Rh(III)-catalysed C–H bond additions to enone-tethered aldehydes (Scheme 2(a)).[13] This reaction begins with concerted metalation deprotonation (CMD) with Rh directed to the *ortho*-position of arene input **1**. Addition to the enone of **2** generates a rhodium enolate that undergoes an aldol reaction with the pendant aldehyde to provide the cyclised product **3** in good yield and with high diastereoselectivity.

While a couple other examples of C–H functionalization with tethered substrates had been reported,[14–16] in their study, Ellman and Boerth next investigated whether the tether between the enone and aldehyde could be removed to achieve an analogous, intermolecular three-component cascade (Scheme 2(b)). Upon decoupling the enone-tethered aldehyde into its respective components, Ellman and Boerth discovered that the resultant multicomponent reaction was highly chemoselective. The initial rhodacycle formed by CMD selectively added to the enone rather than the aldehyde, and the resulting Rh-enolate then underwent an aldol reaction with the aldehyde without competitive Michael reaction with the enone. The authors noted that

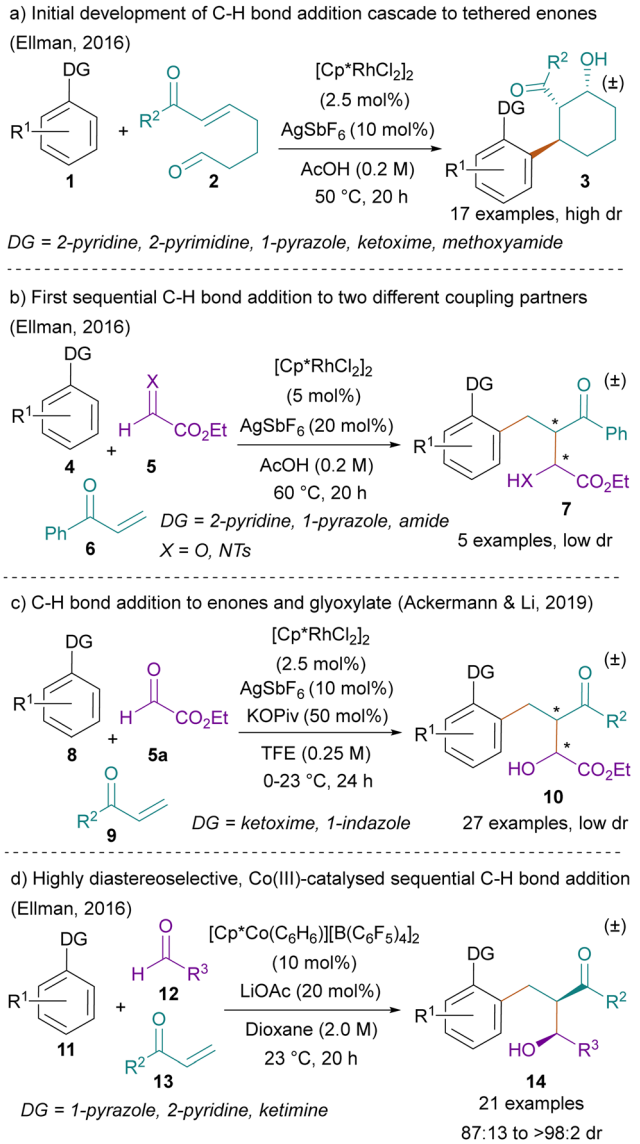

Scheme 2 Development of sequential C–H bond additions to enones and aldehydes.

the chemoselectivity for the initial addition to the enone could either have resulted from kinetic control, with addition to the enone occurring faster than to the aldehyde, or from thermodynamic control, given that C–H bond additions to aldehydes are known to be reversible.[17]

The authors demonstrated preliminary scope for this new type of sequential C–H bond addition reaction, showing that different directing groups could be employed, such as pyridine, pyrazole, and secondary and tertiary amides. However, only the highly electrophilic aldehyde, ethyl glyoxylate, and its tosyl imine derivative, were effective reactants. Moreover, the authors noted that while this reaction was high yielding, poor diastereoselectivity was observed. Nevertheless, this work provided proof of principle that sequential C–H bond addition to two coupling partners could be performed.

In 2019, Ackermann and Li expanded upon this reaction, reporting a similar addition of C–H bonds into different enones and the activated aldehyde, ethyl glyoxylate (Scheme 2(c)).[18] This work also employed Rh(III)-catalysis to perform the same addition, with the benefit of lower catalyst loading as well as neutral conditions relative to the AcOH solvent reported by Ellman. The authors demonstrated an expanded scope of products, with 27 examples employing synthetically useful ketoxime directing groups. They also reported the use of cleavable indazoles as directing groups for coupling of electron-rich thiophene C–H bonds. Finally, the authors reported an expanded enone scope, including alkyl vinyl ketones in addition to aryl vinyl ketones. Despite the expanded scope of this reaction, the diastereoselectivity for the two stereocentres formed was still low, ranging from 1:1 to 3:1 dr.

In 2016, Ellman and co-workers reported much broader aldehyde scope along with high diastereoselectivity for sequential C–H bond additions to enones and aldehydes by employing Cp*Co(III) instead of Cp*Rh(III) catalysis (Scheme 2(d)).[19] They first determined that for less electrophilic aldehydes, addition to the aldehyde did not occur under Cp*Rh(III) catalysis, and instead, direct reaction between the C–H bond substrate and the enone predominated to give alkylation products, likely *via* protodemetalation (*vide infra*). In contrast, the cationic $[Cp^*Co(C_6H_6)][B(C_6F_5)_4]_2$ catalyst[20] enabled aldehyde addition to outcompete enolate protodemetalation, especially at high reaction concentrations.

The reaction proceeded with high diastereoselectivity ranging from 87:13 to >98:2 dr. Both alkyl and aryl enones were compatible. As noted previously, this reaction did not require highly electrophilic glyoxylate aldehydes and instead demonstrated a very broad scope of aryl, alkyl, vinyl, and glyoxylate aldehydes. With respect to directing groups employed, pyrazoles and pyridines were effective, as well as a single example of a ketimine directing group. The authors also demonstrated C–H functionalization of the alkenyl $C(sp^2)$–H bond in **15** (Scheme 3(a)). Upon ozonolysis of the alkene in product **16** followed by treatment with Fétizon's reagent, lactone **17** was obtained with >98:2 dr. Besides reactions with aldehydes, the authors also reported addition to activated *N-tert*-butanesulfinyl imines **18** to enable the asymmetric synthesis of the α-branched amine products **19a** and **19b** (Scheme 3(b)).[21]

Mechanistically, the reaction commenced with a CMD step to form cobaltacycle **I** (Scheme 3(c)). Conjugate addition to the enone furnished enolate **II**. Premature protodemetalation at this step leads to the competing two-component alkylation products observed under rhodium catalysis. However, under cobalt-catalysed conditions, intermediate **II** adds to the aldehyde coupling partner *via* chair-like transition state **III**. Placement of the substituents in the equatorial positions in transition state **III** leads to the observed stereochemical outcome. Protodemetalation then releases product **IV** with regeneration of the Cp*Co(III) catalyst.

Cramer and co-workers further developed C–H bond addition to enones and aldehydes in 2021 by reporting an impressive diastereo- and enantioselective Cp^XCo(III)-catalysed reaction employing a BINOL-derived chiral ligand designed in their lab (Scheme 4(a)).[22] This reaction deviates from previous enolate

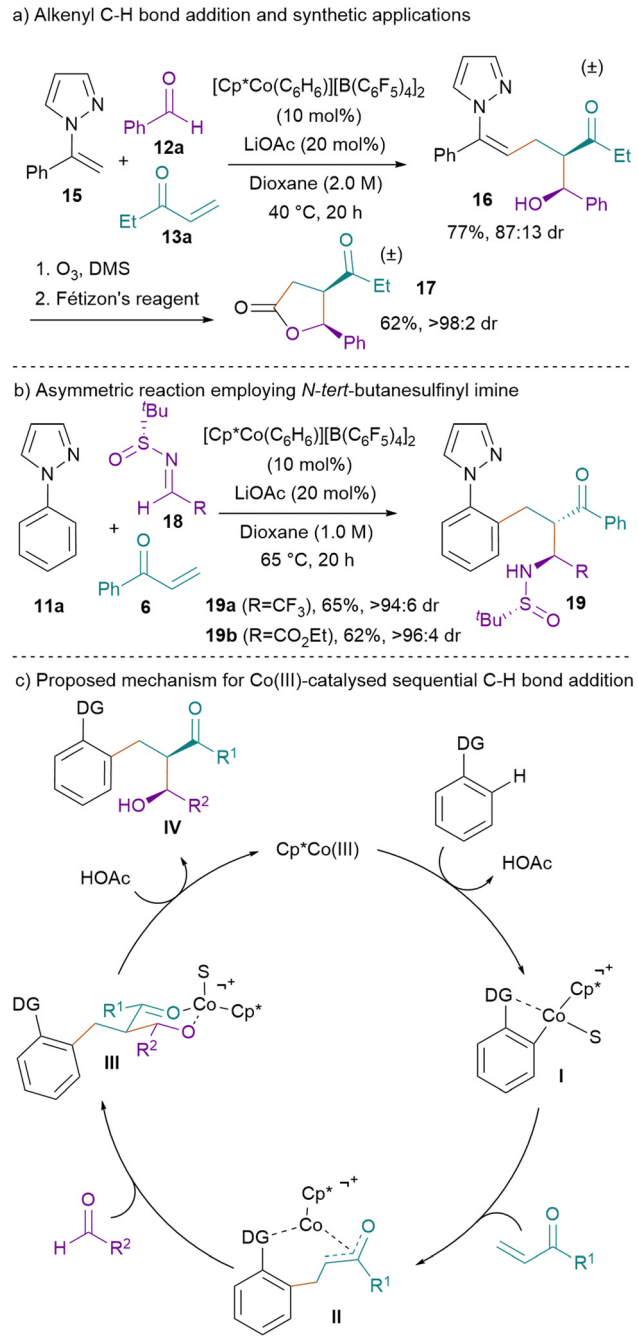

Scheme 3 Applications and mechanism of sequential C–H bond additions to enones and aldehydes.

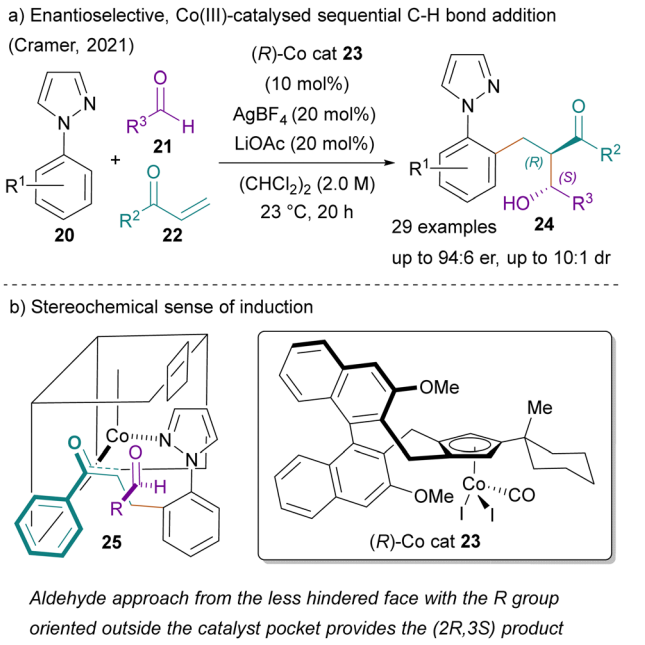

Aldehyde approach from the less hindered face with the R group oriented outside the catalyst pocket provides the (2R,3S) product

Scheme 4 Enantio- and diastereoselective C–H bond addition to enones and aldehydes.

additions into aldehydes in that it selects for a different diastereomer, while also displaying impressive enantioselectivity. The stereochemical control is explained by the model depicted in Scheme 4(b). After CMD, C–Rh bond addition to the enone provides Co-enolate **25**. Due to steric interactions with the Cp^X backbone of catalyst **23**, the authors postulate that the green aryl ring derived from the enone input must be oriented out of the catalyst pocket as depicted. This forces the aldehyde to approach from the top face of the cobalt enolate. The R group on the aldehyde prefers an orientation pointing out of the catalyst pocket to avoid steric interactions. Taken together, the orientation of the cobalt enolate and the approach of the aldehyde lead to the high diastereo- and enantioselectivity observed with the use of this chiral cobalt catalyst. This method is complementary to the previous cobalt-catalysed method for addition to enones and aldehydes because it reverses the diastereoselectivity of the aldol reaction by altering the relative orientation of the Co(III)-enolate and aldehyde in the transition state. Moreover, this transformation highlights that a bulky chiral ligand can have a pronounced influence on aspects of reactivity and stereoselectivity beyond enantioselectivity.

Cramer's enantioselective reaction displays good scope with respect to the aldehyde coupling partner, and is compatible with aryl, aliphatic, and vinyl aldehydes. Enones with various aryl substituents (including those with great steric bulk) could be employed. Ethyl vinyl ketone was employed as an aliphatic enone but showed a lower diastereoselectivity of 2:1. Different aryl pyrazoles were used as C–H bond substrates with high selectivity. However, R^1 groups at the *ortho*-position led to lower selectivity, and the use of an indazole directing group provided no enantioselectivity.

In 2017, Huang, Wang and co-workers described a bimetallic approach for the carboxygenation of enones with C–H bonds and TEMPO, representing the first sequential multicomponent C–H addition reaction to form a new C–O bond (Scheme 5(a)).[23] This reaction was shown to be effective for different N-heterocyclic directing groups such as pyrimidine, pyridine and pyrazole. Various alkyl and aryl enones were compatible, as was acrolein, which led to aldehyde-containing products. The carboxygenation products **29** are of synthetic value given that the 2,2,6,6-tetramethylpiperidine (TMP) functionality present in the products can be readily cleaved under reductive conditions

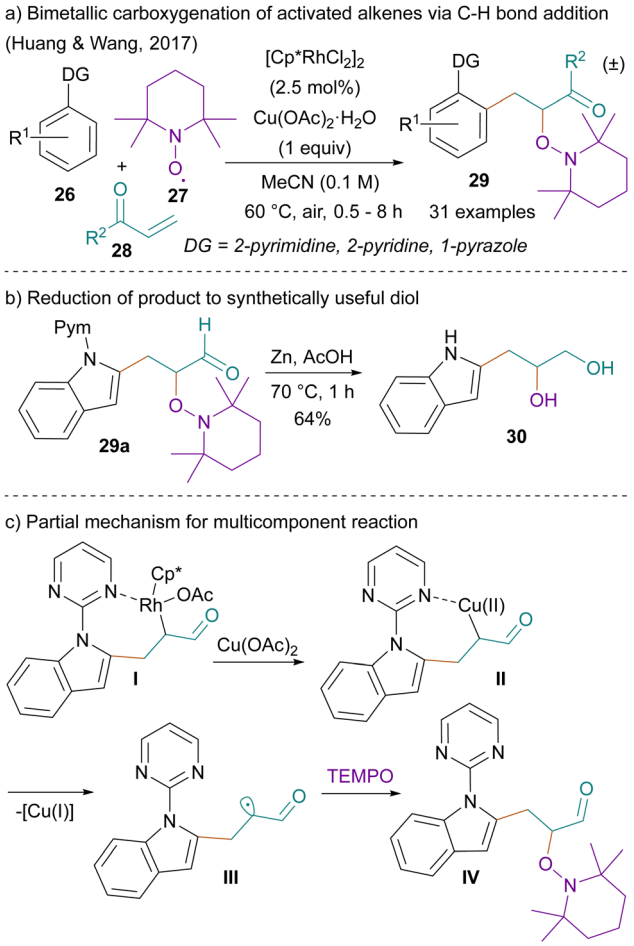

Scheme 5 Bimetallic C–H bond addition to enones/enals and TEMPO.

to provide useful diol products, as exemplified for the conversion of **29a** to **30** (Scheme 5(b)). The authors noted that under the reductive conditions, the pyrimidine directing group was also cleaved.

The authors propose a mechanism for this transformation that occurs first *via* CMD and enone insertion to provide intermediate **I** (Scheme 5(c)). Here, in a mechanistic step unique among sequential C–H bond addition reactions, transmetalation occurs with the copper additive to provide cupracycle **II**. This intermediate then undergoes homolysis to give Cu(I) and the alkyl radical **III**, which is trapped by TEMPO to provide the desired product **IV**. The authors note that this reaction required significant optimisation to avoid unwanted reactivity; for example, when run in protic solvents, protodemetalation of **I** or **II** led primarily to the two-component alkylation product. Similarly, the use of other solvents such as DMF led to unwanted β-hydride elimination of **I** or **II** to provide the undesired two-component alkenylation product.

2.2. Dienes as coupling partners

In their seminal 2018 work, Ellman and co-workers introduced dienes as a coupling partner for sequential Co(III)-catalysed C–H bond addition (Scheme 6(a)).[24] In this work, C–H bonds were added to dienes (including butadiene, 1-substituted and 1,1-terminally disubstituted dienes) and aldehydes. The reaction was highly regio- and diastereoselective with the introduction of up to three new sp^3 and four sp^2 stereocentres, all in >98:2 dr. Perhaps most notable is the synergistic aspect of this reaction. While the three-component reaction proceeds in high yield, neither two-component reaction occurs when the C–H bond substrate is coupled under the standard reaction conditions with either the diene or aldehyde alone.

The reaction enjoyed broad scope with respect to the C–H bond substrate, including secondary, tertiary and Weinreb amide directing groups and different sp^2 C–H bonds, including aryl, hetereoaryl, and alkenyl C–H bonds. The scope of dienes was also broad. The feedstock chemical butadiene was chosen as the standard diene substrate, but terminally substituted butadienes were also used to introduce different alkyl groups besides methyl in the products. Importantly, the *E*/*Z* orientation of these 1-substituted diene inputs did not affect the observed stereochemistry of the product (*vide infra*). Additionally, 1,1-disubstituted butadienes were competent reactants and coupled with high stereoselectivity to provide insight into the reaction mechanism (*vide infra*). However, 1-arylbutadienes were ineffective substrates for this transformation. The scope of aldehydes was very broad. A range of aliphatic and aromatic aldehydes coupled efficiently, including derivatives that incorporated a variety of reactive functionalities such as ketones, esters, primary alkyl chlorides, aryl bromides, and acidic phenols and *N*-Boc anilines.

The mechanism for this transformation begins with a rate-determining CMD to give cobaltacycle **I** (Scheme 6(b)). This species adds across the diene partner to form η^3-Co-allyl complex **II**. Evidence for this step was supported by the isolation and X-ray characterization of this allyl cobaltacycle, which when resubjected to the reaction conditions was a competent catalyst. Next, *syn*-β-hydride elimination followed by *syn*-hydride reinsertion provides η^3-Co-allyl complex **IV**. This species then reacts irreversibly with the aldehyde *via* the chair-like transition state **V** with the aldehyde R group in the equatorial position to furnish product **VI** with the observed stereochemistry after protodemetalation. This mechanism is also consistent with the identical stereochemical outcome observed when (*E*)- or (*Z*)-monosubstituted dienes are employed because they lead to the same intermediate **IV** on the catalytic cycle. Similarly, the high stereoselectivity and relative stereochemistry observed for a 1,1-disubstituted butadiene is consistent with the stereospecific *syn*-hydride elimination and reinsertion proposed as cobaltacycle **II** isomerises to **IV** *via* diene **III**.

The authors noted that the vicinal α-methyl and hydroxyl asymmetric carbons formed in this transformation are a common motif in natural products and sought to demonstrate the synthetic applicability of the method through the synthesis of the Western fragment of the complex ionophore antibiotic lasalocid A **36** (Scheme 6(c)). By coupling benzamide **31a**, butadiene, and isovaleraldehyde, they obtained product **34a** in good yield and selectivity. Product **34a** incorporates the complete carbon framework and key *syn*-α-methyl and hydroxyl groups present in the natural product. Upon alkene hydrogenation,

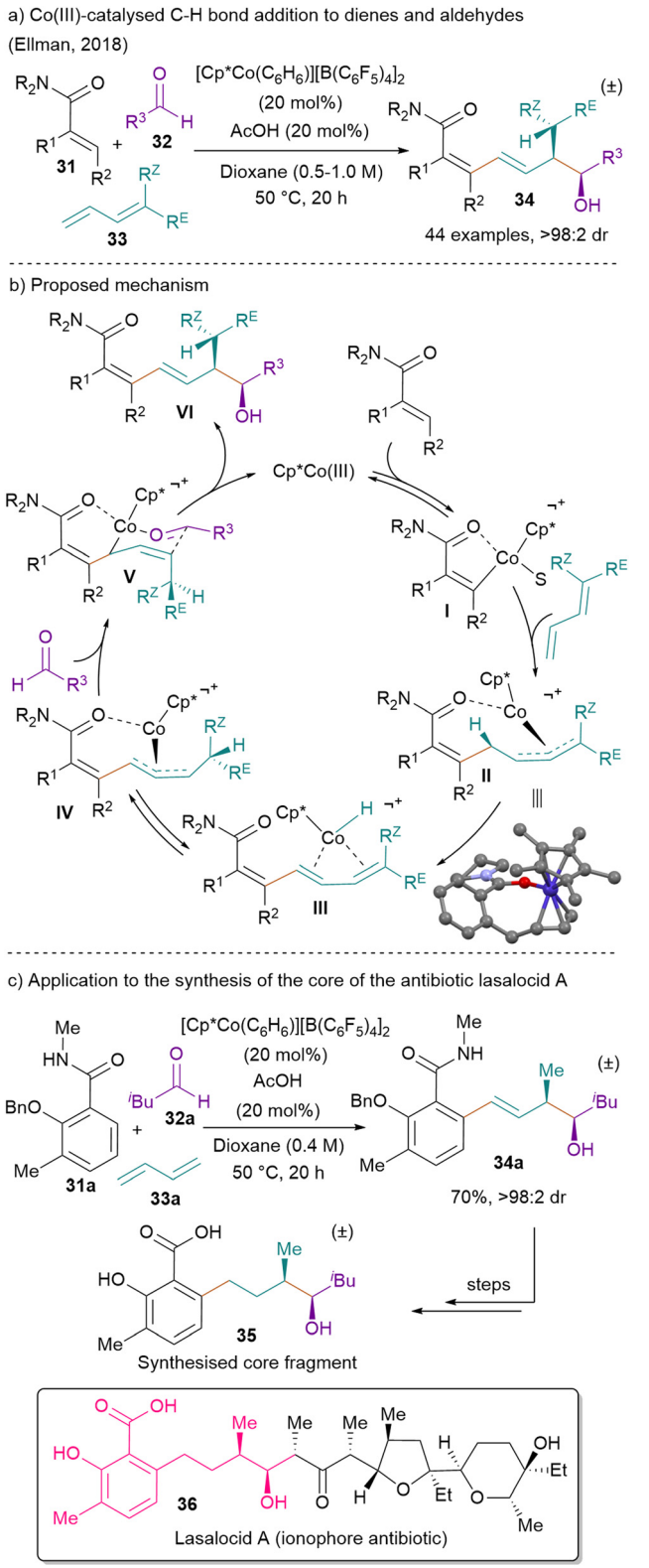

Scheme 6 Additions of C–H bonds to substituted butadienes and aldehydes.

conversion of the amide directing group to the carboxylic acid and benzyl deprotection, they obtained the Western fragment of lasalocid A **35**.

Sequential C–H bond addition to dienes and aldehydes was expanded in 2019 when Zhao and co-workers reported a related coupling of C–H bonds with terminally substituted butadienes and aldehydes, this time using a Rh(III) catalyst (Scheme 7(a)).[25] This work represents a complementary stereoselective approach to homoallylic alcohol products, as it expands the scope of substituted butadienes that can be coupled in such a way. Under cobalt catalysis, aryl butadienes were found to be incompatible, but this Rh-catalysed approach was effective for a range of aryl-substituted butadienes and could also incorporate (in moderate yield) skipped dienes. Additionally, this reaction showed modest reactivity for two internally substituted isoprenes, which foreshadowed later development in the field (*vide infra*). The directing groups for this transformation were limited to N-heterocycles including pyridine, pyrimidine, and pyrazole. The reaction worked best with ethyl glyoxylate as the activated aldehyde coupling partner, though several electron deficient aryl aldehydes could be coupled in good yield when performed with stoichiometric amounts of $Zn(OAc)_2$ and pentafluorobenzoic acid under neat reaction conditions.

This complementary reaction to the cobalt-catalysed work was mechanistically distinct. The authors found, based on KIE studies, that the initial CMD step was not rate limiting. Additionally, the reaction does not occur *via* an intramolecular hydride transfer as in Scheme 6(b), as a 1,1-dideuterated butadiene did not show deuterium migration when subjected to the reaction conditions. Rather, the authors propose that this reaction occurs by protodemetalation followed by allylic C–H activation to give a similar metallacycle to **IV** in Scheme 6(b). Protodemetalation is supported by the observation that when CD_3OD is used as a co-solvent, deuterium incorporation is observed in the product. Like the cobalt-catalysed work, however, the reaction employing rhodium was indeed found to operate synergistically, with neither two-component reaction between the C–H bond substrate and either the butadiene or aldehyde occurring in isolation.

In 2020, Ellman and co-workers expanded the scope of C–H bond additions to butadienes by employing activated ketones as a second coupling partner in place of aldehydes (Scheme 7(b)).[26] This diastereoselective transformation provided homoallylic tertiary alcohols with complete selectivity for the (*E*)-alkene isomer. Ketones had proven to be challenging substrates in previous work due to their inherent stability and steric congestion relative to aldehydes. However, this work showed the effective formation of homoallylic tertiary alcohol products employing cobalt catalysis. The scope of ketones included strain-activated cyclic ketones such as azetidinones, oxetanones, and cyclobutanones. Unsymmetrical, electron-deficient carbonyl derivatives such as cyclic isatins and acyclic ethyl benzoylformate were also effective coupling partners, providing products in >20:1 dr. Finally, the reaction demonstrated a broad scope with respect to directing group, employing secondary and tertiary amides, pyrazoles, and pyrimidines.

In addition to butadienes, Ellman and co-workers demonstrated that internally substituted dienes were effective coupling partners for the synthesis of homoallylic alcohols with acyclic

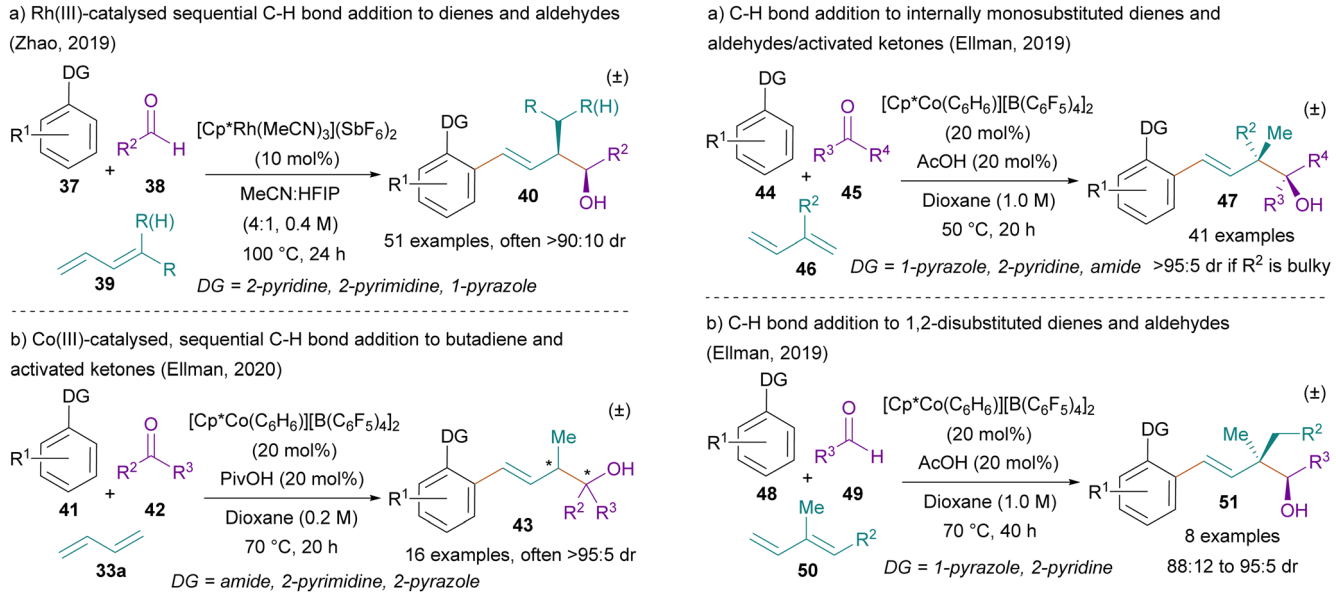

Scheme 7 Additional examples of C–H bond additions to dienes and aldehydes.

quaternary centres (Scheme 8(a)),[27] which can be challenging motifs to prepare.[28–30] In this Co(III)-catalysed work, different 2-alkyl-1,3-butadienes could be employed. When isoprene was used as the internally substituted diene, products containing quaternary geminal dimethyl groups were obtained. Other 2-alkyl-1,3-butadienes were used to stereoselectively provide products with two adjacent stereocentres. These products were typically formed in >95:5 dr, though smaller alkyl substituents or aryl groups on the butadiene led to decreased stereoselectivity. In addition to isoprene inputs, 1,2-disubstituted butadienes could also be employed (Scheme 8(b)). Interestingly, the presence of an R^2 group caused the stereochemistry of the quaternary centre's methyl group to flip relative to when 2-substituted dienes were used (*vide infra*). Here, different alkyl R^2 groups provided products in good dr ranging from 88:12 to >95:5.

With both types of internally substituted dienes, a broad scope of aldehydes and activated ketones was demonstrated. Many different aryl and alkyl aldehydes were used as well as strain activated ketones such as oxetanone, azetidinone, and indantrione. Additionally, electronically activated isatins proved to be effective coupling partners. Finally, this reaction was effective with various directing groups, including pyrazoles, pyridines, and secondary and tertiary amides.

In a related work that was published in the same year, Zhou, Chen and co-workers reported a synthesis of homoallylic alcohols derived from terpenes, using formaldehyde as a hydroxymethylating reagent (Scheme 8(c)).[31] In this work, various terpenes (naturally abundant molecules comprised of isoprene monomer units) were employed as the diene coupling partner, ranging from the simpler myrcene to more complex terpenes such as farnesenol. Notably, this reaction is highly chemoselective, resulting in exclusive functionalization of the terminal conjugated diene of the terpene coupling partner, even in

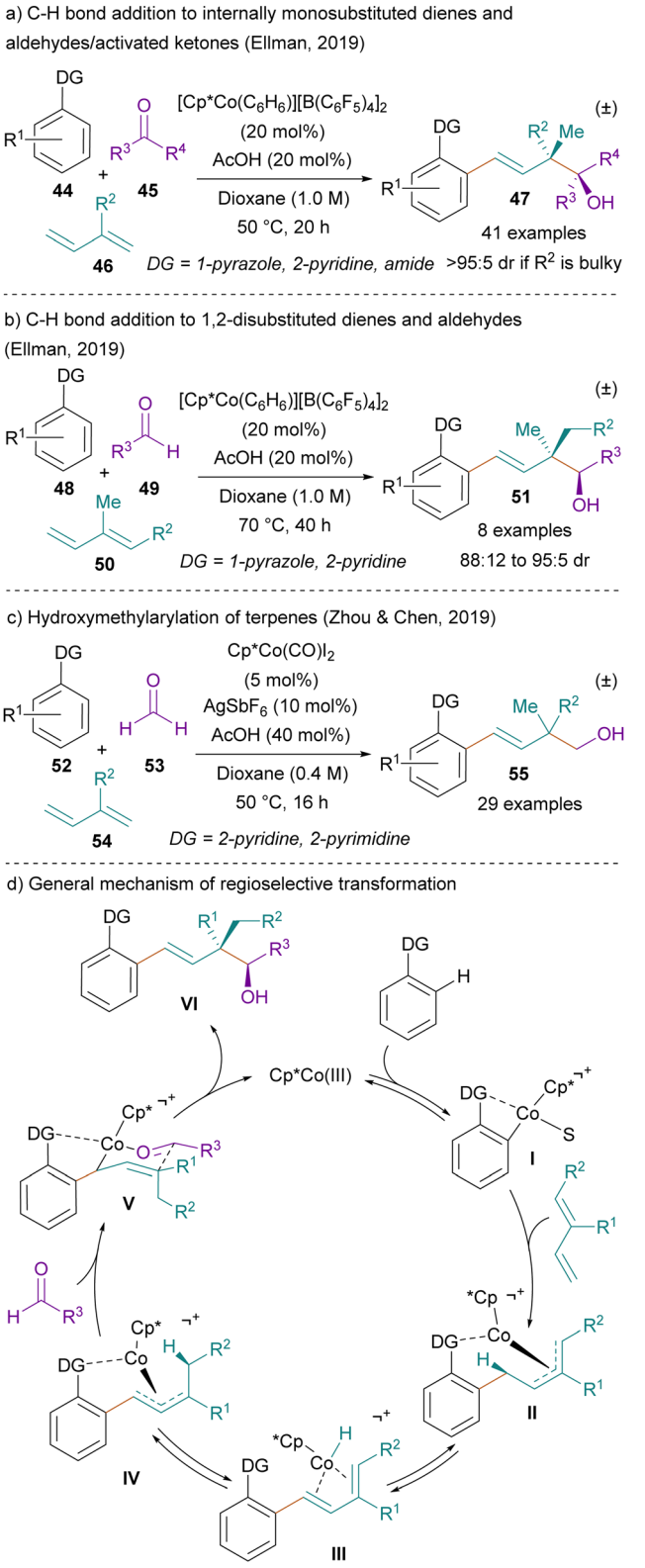

Scheme 8 Additions of C–H bonds to internally substituted dienes and aldehydes.

the presence of multiple other alkenes in the molecule. This selectivity can be attributed both to the enhanced coordinating

ability of the conjugated diene relative to the other terpene π-bonds, as well as the less-hindered steric profile of this diene relative to the trisubstituted alkenes. In this reaction, a simple Co(III) catalyst without a complex counterion could be employed, though the directing group scope was limited to pyridines and pyrimidines.

Similar mechanisms were proposed for both reactions employing internally substituted dienes (Scheme 8(d)). In the presence of a cobalt catalyst, a rate-determining CMD gives cobaltacycle **I**. Coordination and migratory insertion of the diene gives η^3-Co-allyl complex **II**. β-hydride elimination, followed by *syn*-hydride reinsertion provides η^3-Co-allyl complex **IV**, as evidenced by deuterium incorporation studies.[27] Diastereoselective addition of intermediate **IV** to the aldehyde (or activated ketone) proceeds *via* the chair-like transition state **V**. Finally, release of the product **VI** by protonolysis regenerates the catalyst. The observed stereochemical outcomes are consistent with transition state **V**. The R^1 and R^2 substituents must be located in the equatorial and axial positions in the chair-like transition state, respectively, due to their *anti* and *syn* placements in η^3-Co(III)-allyl intermediate **IV**.

Consistent with Zhao's findings that 1-aryl butadienes are competent for Rh(III)-catalysed sequential C–H bond additions with aldehydes (Scheme 7(a)), Glorius[32] and Wang and Li[33] established that these types of dienes are also excellent substrates for regiodivergent Rh(III)-catalysed sequential C–H bond additions to dienes and amidating reagents (Schemes 9 and 10). In 2019, Glorius and co-workers reported a regioselective, three-component 1,4-carboamidation of 1-arylbutadienes (Scheme 9(a)).[32] Here, using a Cp*Rh(III) catalyst, they were able to couple aryl C–H bonds employing Weinreb amide directing groups to 1-arylbutadienes and dioxazolone[34] amidating agents. This method was especially notable for its high regioselectivity, favouring the 1,4-carboamidated products, often in >20:1 dr.

A range of different aryl Weinreb amides containing different functionalities on the aromatic ring, as well as an example of an indole-derived carbamate, and an aryl tertiary amide were employed. Many 1-(hetero)arylbutadienes were also employed, as well as a single example of a 1,3,5-triene coupling partner. *tert*-Butyl dioxazolone was chosen as the optimal amidating reagent due to its steric profile (*vide infra*).

The pronounced regioselectivity of this transformation is understood through examination of the proposed mechanism (Scheme 9(b)). After CMD to form rhodacycle **I**, migratory insertion of the 1-arylbutadiene provides η^3-Rh-allyl complex **II**. Next, insertion of the dioxazolone forms the rhodium nitrenoid **III**, while extruding CO_2. Reductive elimination can then occur, furnishing a new C–N bond, either at the 2- or 4-position of the diene. The regioselectivity is enforced at this step by the bulky *tert*-butyl group, which prefers the less sterically encumbered 1,4-insertion, to give intermediate **IV**. Thereafter, protodemetalation provides product **V** and regenerates the cationic catalyst. The mechanism was supported by various deuterium-labelling studies, in which deuterium migration was not observed for differently deuterated diene inputs.

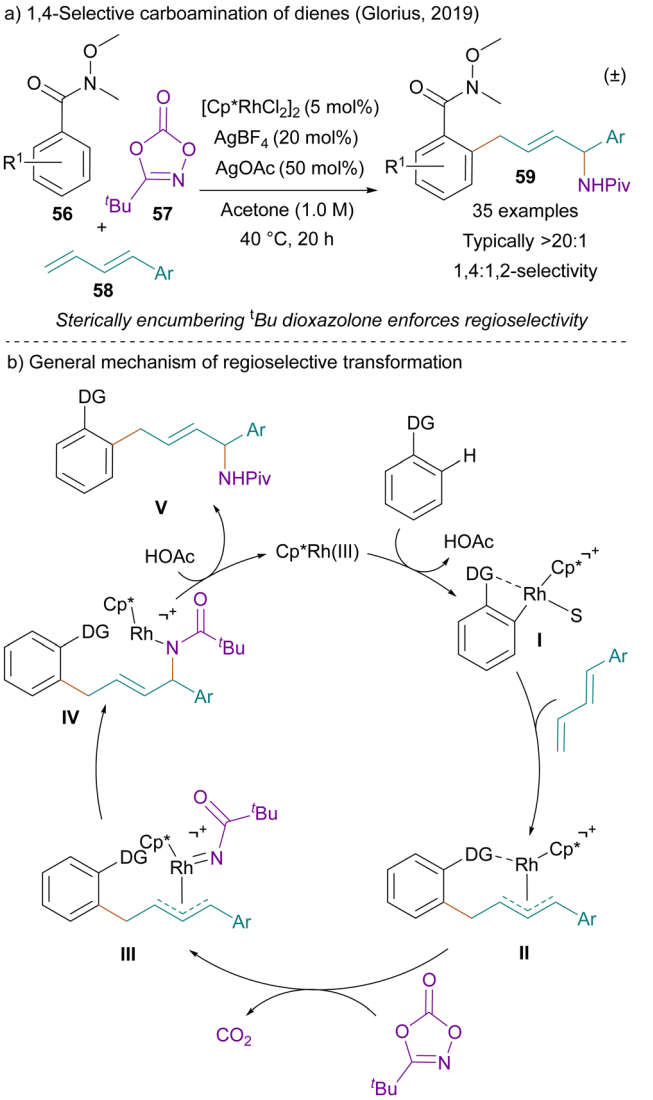

Scheme 9 Sequential C–H bond addition to 1-arylbutadienes and amidating reagents.

The rationale for the 1,4-selectivity was supported by reaction with the smaller methyl dioxazolone, which provided a 1 : 1.6 ratio of 1,4 : 1,2-carboamidated products, consistent with the hypothesis that steric interactions were important for the high regioselectivity of the reaction.

In 2021, Wang, Li and co-workers expanded on Glorius' work in describing a complementary enantio- and 1,2-regioselective carboamidation[33] using a Rh(III) catalyst employing a BINOL-derived chiral Cp ligand[35] developed by Cramer (Scheme 10(a)). Wang and Li reported a highly enantioselective reaction with up to 99% ee, and exclusive regioselectivity for the 1,2-carboamidated product.

The major points of differentiation between this work and Glorius' example are the use of smaller alkyl dioxazolones and bulky pyrrolidine benzamide C–H bond reactants. Like the previous example, this reaction proceeds first *via* a rate limiting CMD, followed by diene insertion (Schemes 9(b) and 10(b)).

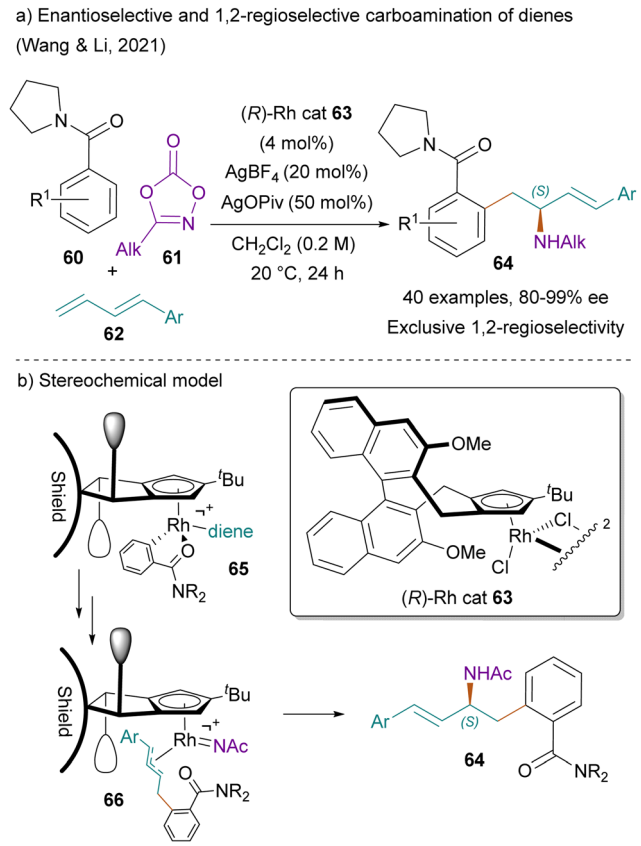

Scheme 10 Regio- and enantioselective 1,2-carboamidation of dienes.

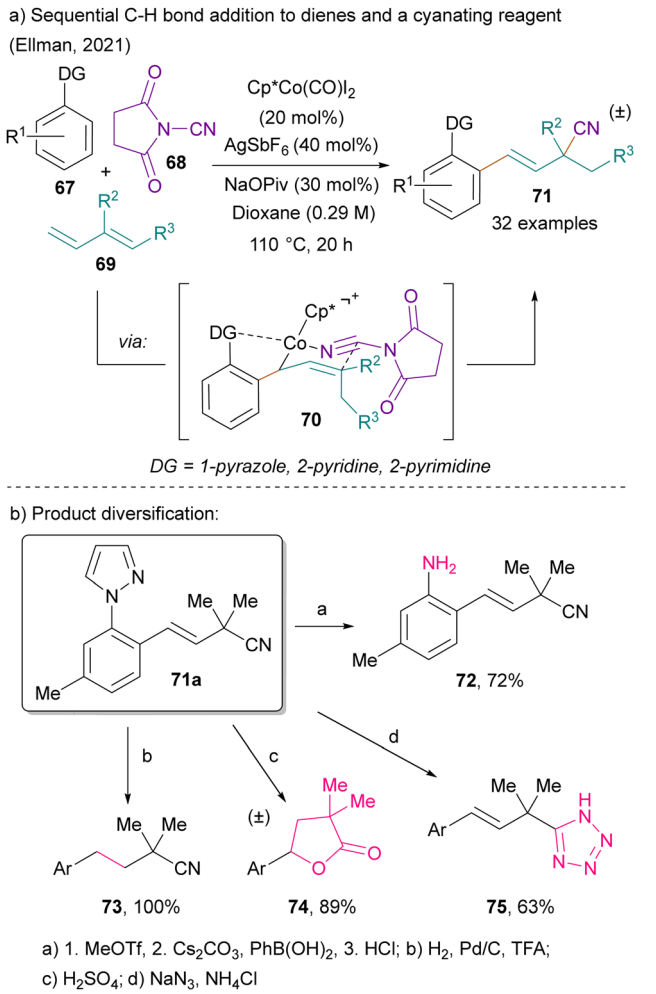

Scheme 11 Sequential C–H bond addition to dienes and a cyanating reagent.

It is notable that for both 1,4- and 1,2-amidations, two-component amidations represent competing reactivity; therefore, the migratory insertion of the diene into the rhodacycle must outcompete direct amidation. Formation of the Rh(v) nitrenoid **66** enables a reductive elimination to provide the 1,2-carboamidation product **64** (Scheme 10(b)). Based on DFT calculations with a Cp*Rh(III) catalyst, Wang and Li attribute the preference for the 1,2-regioisomer to high-energy steric interactions between the methyl group in the Rh(v) nitrenoid intermediate derived from a methyl dioxazolone and the bulky pyrrolidine benzamide in the alternative 1,4-addition pathway.

Wang and Li also propose a stereochemical model to explain the enantioselectivity achieved using the chiral ligand (Scheme 10(b)). In the model, the bulky amide directing group is oriented out of the steric pocket created by the chiral ligand. Thus, after migratory insertion and nitrene formation, **66** is oriented with the allyl group to the back as depicted. Amination therefore occurs at the Si face of the π-allyl complex, affording the observed (*S*)-product.

The reaction was primarily explored with bulky amide directing groups and for these systems is compatible with many different electronically modulating substituents at all positions of the aryl ring of the C–H bond substrate. Various 1-aryl dienes were employed with different substituents at all positions of the arene. Finally, different small alkyl dioxazolones were used while retaining 1,2-selectivity, including methyl, *n*-hexyl and *n*-heptyl dioxazolones.

In 2021, Ellman and Dongbang reported the use of *N*-cyanosuccinimide as a third component for cyanative coupling with C–H bond substrates and dienes (Scheme 11(a)).[36] The introduction of a nitrile group was an important contribution to this field given the nitrile's ubiquity in natural products, pharmaceuticals, agrochemicals, and materials,[37,38] as well as its importance as a synthetic intermediate.[39–41] *N*-Cyanosuccinimide, an electrophilic cyanating reagent, was chosen as a way to avoid the use of toxic cyanide sources.[42,43]

This reaction is mechanistically related to sequential Co(III)-catalysed additions to dienes and carbonyl compounds because the nitrile group is introduced at the 3-position of the diene *via* a β-hydride elimination/reinsertion process to generate the reactive Co-allyl intermediate (Scheme 11(a)). The *N*-cyanosuccinimide is proposed to coordinate to the Co-allyl species in a chair-like transition state, promoting addition into the electrophilic carbon of the nitrile.[44] A very broad range of dienes were effective inputs for this transformation. Isoprenes and other internally substituted dienes coupled efficiently, and even internally aryl-substituted dienes could be employed whereas they were incompatible with previous chemistries. 1,2-Disubstituted dienes were

also effective substrates, including for both 1-alkyl- and 1-aryl-substituted dienes. Finally, tertiary centres could be synthesised employing butadiene and 1,3-pentadiene. With such a broad diene scope, various products **71** with quaternary (and tertiary) centres were prepared. In addition to the diene scope, this chemistry was effective for various N-heterocyclic directing groups, including pyrazole, pyridine, and pyrimidine.

Nitrile **71a** was then converted to several distinct types of compounds to demonstrate the synthetic versatility and utility of this class of sequential C–H bond addition products (Scheme 11(b)). For the preparation of **72**, the authors developed a convenient new method for converting the frequently used pyrazole directing group to the aniline[45] by pyrazole *N*-methylation and hydrolysis. Hydrogenation of the alkene provided the saturated congener **73** in quantitative yield. Hydrolysis of the nitrile and *in situ* cyclisation provided γ-lactone **74** in high overall yield. Finally, the authors demonstrated straightforward conversion of the nitrile **71a** to tetrazole **75**. Synthesis of the tetrazole is relevant to potential drug discovery applications because this motif is prevalent in drugs and drug candidates.[46]

2.3. Enynes as coupling partners

In 2022, Ellman and co-workers demonstrated the utility of enynes as an effective coupling partner for sequential C–H bond addition with aldehydes to provide allenyl alcohols **79** with high stereoselectivity (Scheme 12(a)).[47] This was the first example of C–H bond addition to 1,3-enynes to give allenyl alcohol products. Allenyl alcohols are versatile scaffolds for varied processes such as elimination, substitution and rearrangements, and cyclisation.[48–50]

Several challenges were overcome to achieve the desired synthesis of allenyl alcohols, including promoting reactivity of the alkene over the inherently more reactive alkyne portion of the 1,3-enyne. To solve this problem, a bulky silyl group was placed at the alkynyl position to encourage addition to the distal alkene. Another challenge was the competing synthesis of undesired homopropargylic alcohols *via* metallotropic equilibria between propargyl/allenyl metal species. This problem in regioselectivity was solved by the use of a basic additive instead of the acidic additives often employed in Co(III)-catalysed C–H bond additions.

This reaction showed a wide aldehyde scope, including both alkyl and aryl aldehydes, often with good diastereoselectivity. The most effective C–H bond substrates were electron rich heteroaromatics with amide directing groups as exemplified by thiophene and furan derivatives. Additionally, less electron-rich aryl substrates such as 2-phenylpyridine and an aryl pyrazole were employed, albeit with more modest yield and dr. The enyne scope was also demonstrated, though these coupling partners required bulky alkynyl-substituents such as silyl or *tert*-butyl groups to reduce undesired direct addition to the alkyne. The bulky allenyl silyl group was removed in a two-step sequence including a Brook rearrangement to the silyl alcohol under basic conditions, followed by alcohol

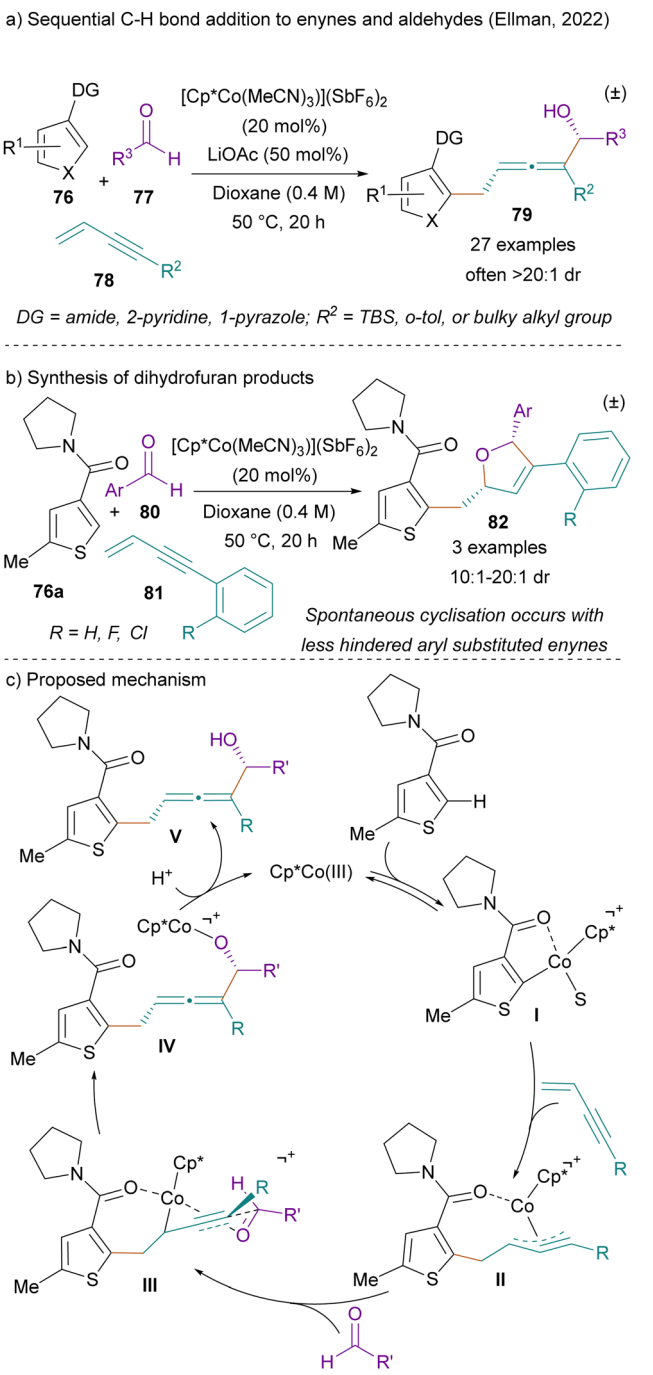

Scheme 12 Synthesis of allenyl alcohols from enyne coupling partners.

deprotection with TBAF. Attempts at direct allene desilylation resulted in a complex mixture of diastereomers.

Notably, when the alkynyl position contained a less hindered aryl substituent, stereoselective formation of dihydrofuran products **82** was observed due to spontaneous cyclisation of the initial allenyl alcohol product (Scheme 12(b)). This process could be facilitated by the incorporation of an *ortho*-halogen on the alkynyl arene, which was hypothesized to coordinate to the Lewis acidic Co to facilitate chelation to the allene and catalyse cyclisation. When bulkier alkynyl substituents were

employed, the authors demonstrated that cyclisation of the allenyl alcohol to the dihydrofuran could be achieved stepwise and in good yield by treatment with $AgNO_3$.

Mechanistically, this reaction proceeds *via* CMD, followed by enyne insertion to provide η^3-Co-propargyl complex **II** (Scheme 12(c)). Addition of the aldehyde to **II** *via* the half-chair transition state **III** provides the observed stereochemical outcome in **IV**. The aldehyde R′ substituent must point away from the Co centre due to steric interaction with the bulky Cp* ligand, as well as the alkyne R group. This orientation leads to the observed diastereoselective outcome. Protonolysis then provides the final product **V** and regenerates the catalyst. The proposed mechanism was supported by isolation of different cobaltacycles **II**, which when resubjected to reaction conditions, provided products in similar yield and selectivity to the standard catalyst.

3. Sequential C–H bond addition reactions employing isolated π-systems as the first coupling partner

3.1. Alkynes and allenes as coupling partners

In 2017, Ellman and Boerth reported on the three-component Co(III)-catalysed synthesis of alkenyl halides from aryl and heteroaryl C–H bond substrates, terminal alkynes (and allenes), and halogenating agents (Scheme 13(a)).[51] This reaction was highly regio- and diastereoselective, providing single isomers of alkenyl halide products **86**. Notably, alkenyl halides are attractive inputs for various chemistries including many transition metal-catalysed transformations.[52–54]

Upon C–H activation by CMD, addition to the alkyne must outcompete direct halogenation by the electrophilic halogenating reagent, which is documented to be a facile Co(III)-catalysed transformation.[55] Other possible side reactions included terminal alkyne homocoupling, oligomerisation, and competitive protodemetalation leading to two-component alkenylation.[56–58] The authors report the use of a Cp*Co(III) catalyst as being critical for the successful reaction, while other group IX metals were ineffective. Additionally, a catalytic amount of acetic acid as an additive resulted in a significantly higher product yield.

The terminal alkyne scope was broad, with a wide range of aryl and aliphatic terminal alkynes, including those displaying different functionality, such as a Boc-protected amine, an ester, and protected alcohols. Different (hetero)aromatic C–H bond substrates with amide and pyrazole directing groups were employed. *N*-Bromosuccinimide (NBS) and *N*-iodosuccnimide (NIS) were effective for the preparation of alkenyl bromides and iodides, respectively, but the authors were not able to access the corresponding chloroalkenes. Finally, terminal allenes could be employed in place of terminal alkynes to regioselectively provide tetrasubstituted alkenyl iodides *via* haloarylation across the terminal π-system of the allene (Scheme 13(b)).

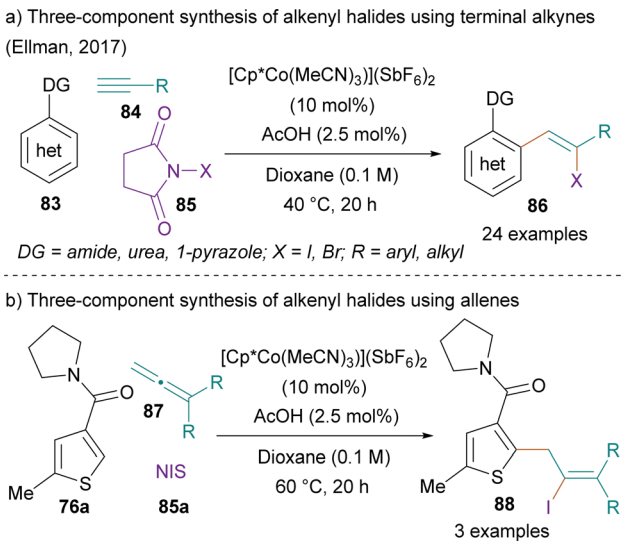

Scheme 13 Sequential C–H bond addition to prepare alkenyl halides.

3.2. Alkenes as coupling partners

In 2019, Ellman and co-workers developed a new approach for sequential Rh(III)-catalysed C–H bond addition to terminal alkenes and electrophilic aminating reagents (*O*-acyl hydroxamic acids[59–61] and dioxazolones[34]) to provide α-branched amines either as carbamate **92** or amide **96** products (Scheme 14(a) and (b)).[62] This modular approach creates the α-branched amine products in one step, installing a stereocentre by the sequential formation of new C–C and C–N bonds. α-Branched amines represent an important target for synthesis given their prevalence in drugs and drug candidates.[63]

The authors demonstrated a broad scope for all three reactants. The *O*-acyl hydroxamic acid aminating reagents directly provided amines with the most common protecting groups such as Boc, Cbz, Fmoc and Tosyl pre-installed (Scheme 14(a)). On the other hand, dioxazolones were used to prepare a variety of alkyl, aryl and (hetero)aryl amides (Scheme 14(b)). Many aryl and heteroaryl C–H bond substrates were employed, including with a range of directing groups such as amides, oximes, pyridine, pyrimidine, pyrazole, and triazole.

The authors extensively evaluated the terminal alkene scope. Alkyl alkenes, styrenes, and α,β-unsaturated esters were all effective coupling partners. Moreover, a large variety of functional groups were incorporated in the alkene and shown to be compatible, including electrophilic functionalities like primary alkyl chlorides, epoxides, aldehydes, ketones and esters, and acidic functionalities such as alcohols and protected amines. Importantly, the feedstock commodity chemicals ethylene and propylene were effective reactants, with ethylene being of particular value because it enabled the synthesis of α-methyl amines, which are present in a wide range of pharmaceuticals.

The authors performed the reaction enantioselectively with Rh catalyst **97** bearing the first-generation chiral BINOL-derived ligand developed by Cramer and co-workers (Scheme 14(c)).[64] Though the observed enantioselectivity was relatively modest (72–84% ee), the use of later-generation ligands of this class might be expected to lead to enhanced selectivity.[35,65–67] Finally, the authors prepared multiple different products at

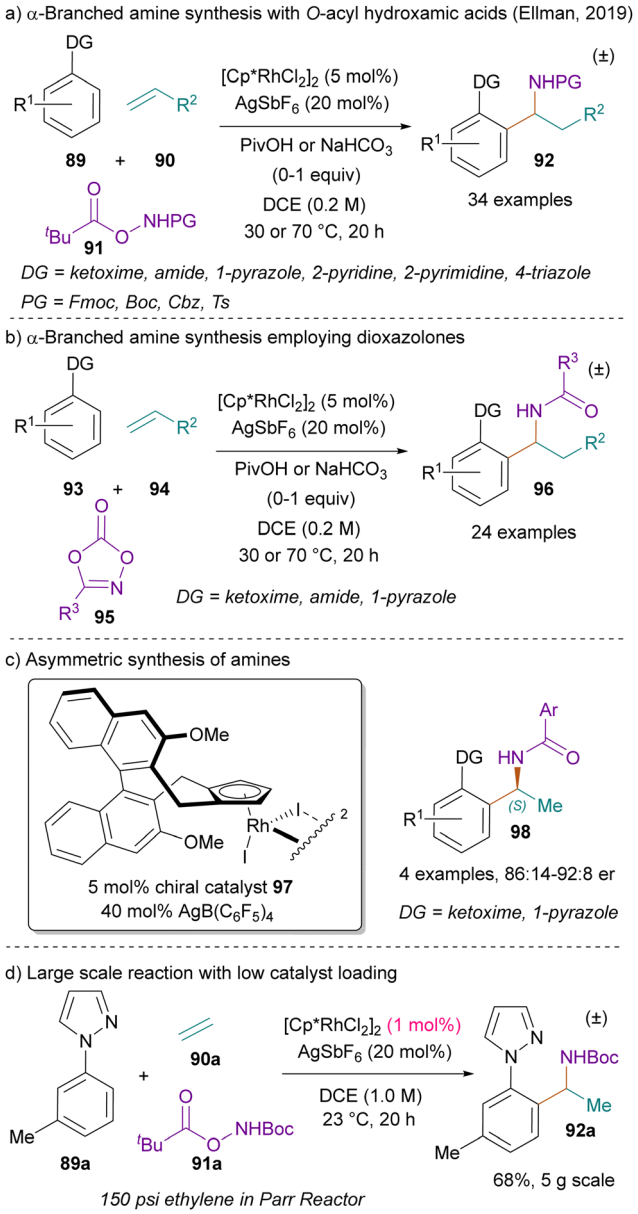

Scheme 14 Sequential C–H bond addition to alkenes and electrophilic aminating reagents for the synthesis of α-branched amines.

1% loading of $[Cp^*RhCl_2]_2$, including for the feedstock gas ethylene on a large scale with a Parr reactor (Scheme 14(d)).

A unique mechanism was proposed for this reaction (Scheme 15). Reversible CMD provides rhodacycle **I**. Migratory insertion of the terminal alkene then gives the seven-membered rhodacycle **II**. A *syn*-β-hydride elimination occurs to generate the Rh–H complex **III**, which undergoes a *syn*-hydride reinsertion to the distal carbon position, furnishing the six-membered rhodacycle **IV**. The stereospecific nature of the *syn*-β-hydride elimination/reinsertion step was verified by deuterium labelling studies. Here, different stereospecifically labelled deuterated styrenes each led to the formation of α-branched amine products as single stereoisomers, an outcome that could only be explained by *syn*-elimination and *syn*-reinsertion.

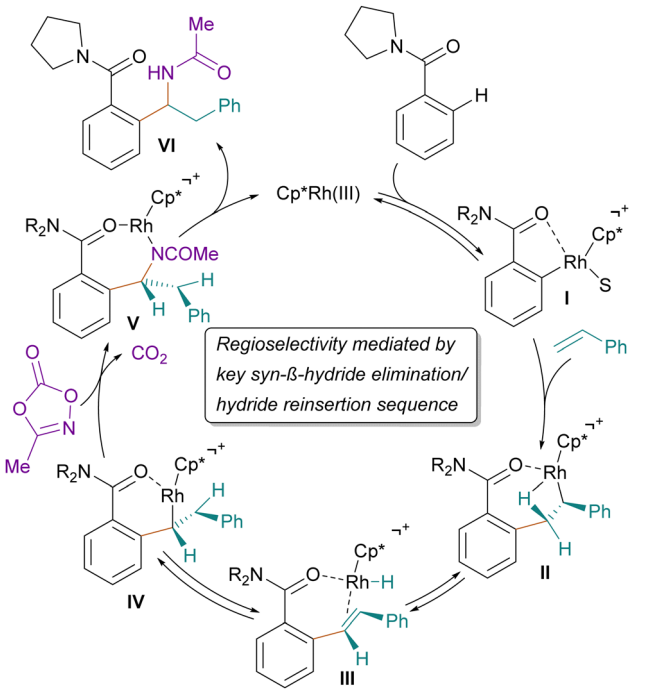

Scheme 15 Mechanistic rationale for 1,1-carboamidation.

This step has important implications as it sets the eventual 1,1-regiochemistry of the final product by favouring the six-membered rhodacycle **IV** over the initial seven-membered rhodacycle **II**. Coordination of the amidating agent followed by nitrene insertion provides **V**, which upon protodemetallation provides the product and regenerates the cationic active catalyst.

Cp*Rh(III)-catalysed syntheses of all three possible two-component side products have been reported. C–H bond substrates couple efficiently with alkenes[6,68] and amidating reagents,[61] and alkenes undergo allylic amidation with dioxazolones.[69–71] It is remarkable that formation of the three-component product can outcompete the three possible two-component reactions under these conditions.

In 2021, Ellman and co-workers reported a related study on the three- and four-component synthesis of α-branched amines employing a readily-diversifiable hydrazone directing group (Scheme 16(a)).[72] They prepared similar branched amide products to their previous paper, but employed a synthetically tractable directing group. While many commonly employed directing groups for group IX metal catalysis (*i.e.* basic N-heterocycles, amides) require specialised or harsh conditions for their elaboration, the authors employed aldehyde-derived *N*,*N*-dialkyl hydrazones, which can be cleaved to form a variety of value-added products under mild conditions. Moreover, hydrazones are an attractive choice for directing group as they are easily accessed by the condensation of hydrazines and aldehydes, of which huge numbers are commercially available.

This method also enabled the development of a rare example of a four-component reaction that incorporates C–H functionalization. The authors determined that hydrazone condensation could be performed *in situ* when the relatively acidic solvent HFIP

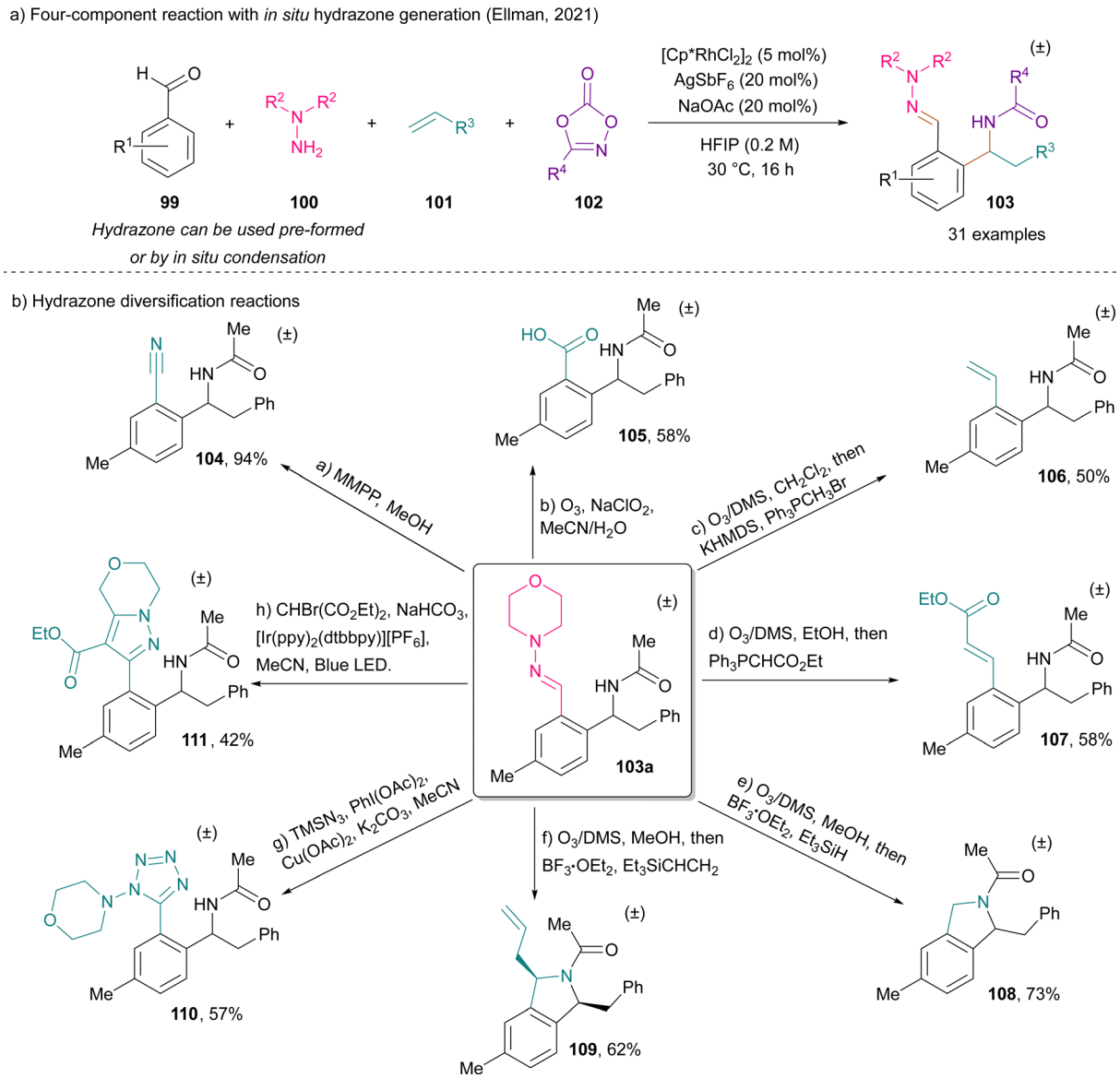

Scheme 16 Three- and four-component carboamidation employing a readily diversifiable hydrazone directing group.

was used. Similar yields were observed for the four-component reaction and the corresponding three-component reaction where the hydrazone was pre-formed. Broad scope was observed for alkene and dioxazolone coupling partners, including both aliphatic and aryl alkenes and dioxazolones. Different dialkyl hydrazones could also be employed.

In this reaction, two-component reactivity competed with the formation of the desired three- and four-component products. For example, with excess of dioxazolone, two-component C–H amidation was observed to be a significant side-product, again illustrating the point that in sequential multicomponent additions, off-target reactivity must often be considered.

Hydrazone product **103a** was then converted to a variety of different compounds under mild conditions utilising both heterolytic and homolytic chemistries (Scheme 16(b)). Treatment of **103a** with the mild oxidant MMPP generated the nitrile **104**. In contrast, under oxidative ozonolysis conditions, the carboxylic acid **105** was formed. Under reductive ozonolytic conditions, the aldehyde was in equilibrium with the hemiaminal generated by attack of the proximal amide; however, the hemiaminal retained aldehyde reactivity, and could be converted to various alkenes in a one-pot, two-step sequence. Accordingly, ozonolysis of the hydrazone gave the aldehyde/hemiaminal mixture that without isolation was submitted to Wittig reactions to generate alkenes **106** and **107**. Upon treatment with boron trifluoride etherate and a hydrosilane or allylsilane, the hemiaminal was converted to isoindolines **108** and **109**, respectively. Additionally, the hydrazone could be converted to biomedically relevant heterocyclic motifs *via* single-electron processes. Under homolytic Cu(II) radical chemistry, a morpholine-substituted tetrazole **110** was generated, and under photoredox conditions, the bicyclic pyrazole **111** was prepared. These results point to the hydrazone as a highly

versatile directing group for sequential C–H bond additions as well as for other C–H functionalization reactions.

The use of terminal alkenes as coupling partners in Rh(III)-catalysed carboamidations led exclusively to 1,1-substitution patterns due to the observed *syn*-β-hydride elimination/reinsertion depicted in Scheme 15. In 2021, Ellman and co-workers reported on a regiodivergent 1,2-carboamidation reaction where new C–C and C–N bonds were formed on different carbon centres through the use of bridged bicyclic alkenes as the second component to give bridged bicyclic products **115** (Scheme 17(a)).[73] This reaction furnishes interesting elaborations of [2.2.1]- and [3.2.1]-bridged bicyclic compounds, which are common scaffolds in drugs and drug candidates.

A wide range of bicyclic alkenes could be employed, including norbornene, and benzonorbornadiene and its congeners containing nitrogen and oxygen bridges. Additionally, a tropinone-derived [3.2.1]-bicyclic alkene was found to be an effective substrate to access products of larger ring sizes. A broad scope was exhibited with respect to C–H bond substrates containing various directing groups, including amides, a pyrazole and a triazole. Additionally, the dioxazolone scope yielded a wide range of both aryl and aliphatic amide products. Finally, the first-generation chiral catalyst **97** developed by Cramer was again employed to demonstrate enantioselectivities ranging from 80–84% ee (Scheme 17(b)).

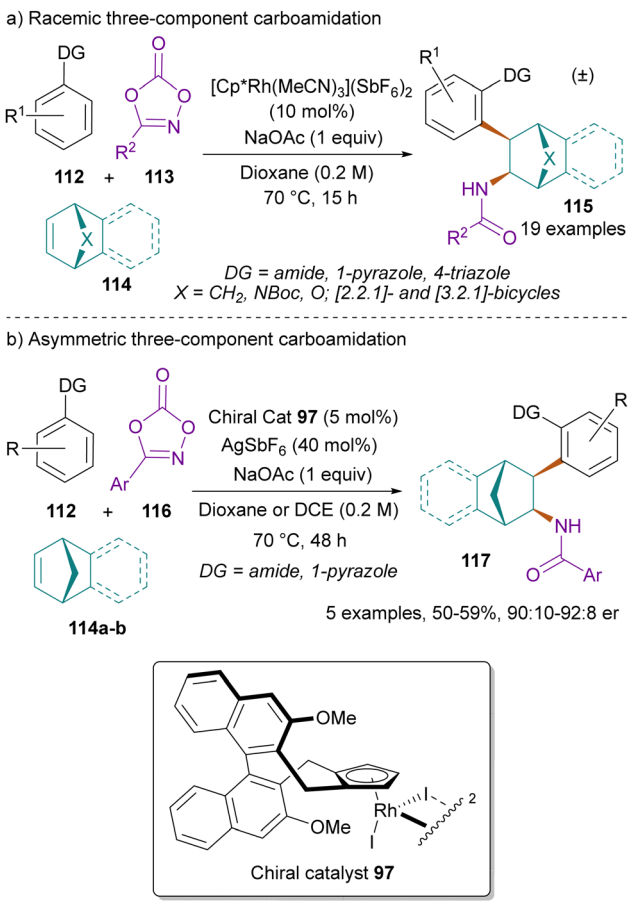

Scheme 17 Three-component carboamidation of bridged bicyclic alkenes.

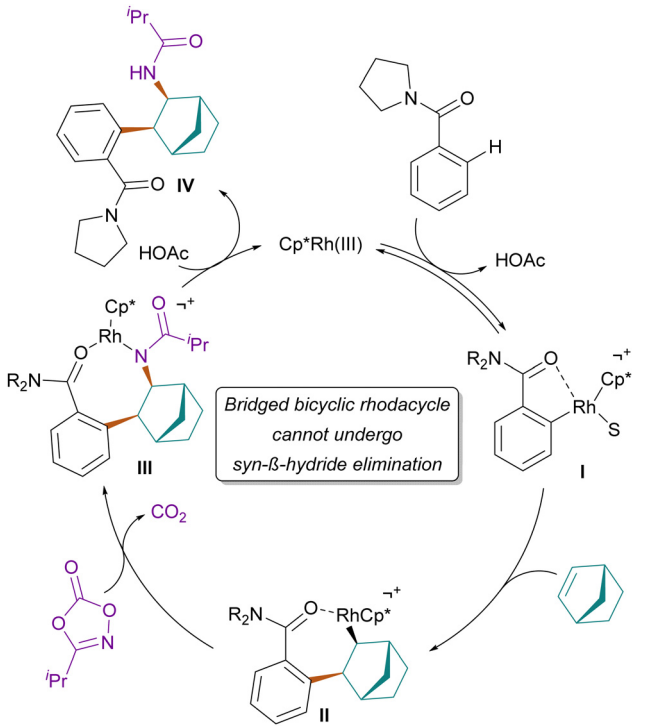

Scheme 18 Mechanistic rationale for 1,2-carboamidations of bridged bicyclic alkenes.

Mechanistically, this reaction occurs *via* an analogous pathway to the prior syntheses of α-branched amines (Scheme 18). First, CMD provides the rhodacycle **I**, into which the bridged bicyclic alkene undergoes migratory insertion to give rhodacycle **II**. This intermediate, by contrast to the reaction using terminal alkenes, does not undergo a *syn*-β-hydride elimination. Due to the locked configuration of the bicyclic scaffold, the key β-C–H bond is oriented *anti* to the C–Rh bond, and therefore cannot participate in the required agostic orbital interactions to achieve a *syn*-β-hydride elimination.[74] Similarly, the bridgehead C–H bond cannot undergo β-hydride elimination as that would lead to the energetically unfavourable anti-Bredt alkene. As a result of these physical constraints, the metal centre does not migrate carbons, and nitrene insertion occurs directly to give **III**, which then provides the 1,2-carboamidation product **IV** after protodemetalation.

In this reaction, the conditions needed to be fine-tuned to prevent undesired side-products. For example, under acidic conditions, two-component C–H alkylation products predominated, whereas basic additives enabled the exclusive formation of three-component products. Additionally, the use of aryl dioxazolones often necessitated milder conditions to prevent competing overaddition products, where a second CMD would occur on the newly installed aryl amide.

That this chemistry was compatible with heteroatomic-bridged alkene substrates (for example, *N*-Boc azabenzonorbornadiene) was notable: under transition-metal catalysed conditions, these substrates typically undergo ring opening reactions, pioneered by Lautens and co-workers.[75] That the bridged bicyclic

scaffold was retained under these conditions speaks to the mild nature of these Rh(III)-catalysed conditions. Indeed, when employing the bulky BINOL-derived chiral catalyst, heteroatom-bridged alkenes could not be employed, likely due to ring opening and non-productive catalyst complexation.

3.3. Bicyclobutanes as strain-activated π-bond isosteres

In 2021, Glorius and co-workers expanded the chemical space of the first coupling partner by introducing bicyclo[1.1.0]butanes (BCBs) **119** as a strain activated π-bond isostere (Scheme 19(a)).[76] They hypothesized that the release of the high strain energy associated with these coupling partners would enable them to insert into key C–Rh bonds analogously to the various π-bond systems described previously. This chemistry, employing a C–H bond substrate, BCB esters, and ethyl glyoxylate, was shown to provide complex products **120** containing challenging quaternary carbon centres with high diastereoselectivity.

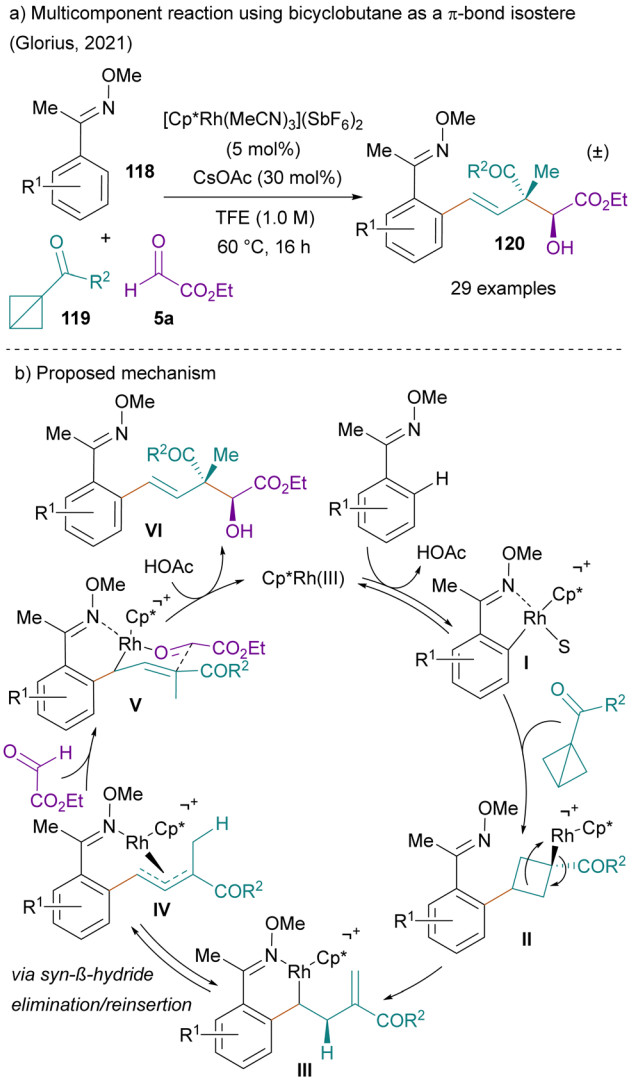

Scheme 19 Sequential C–H bond addition to bicyclobutanes and ethyl glyoxylate.

In the reported Rh-catalysed reaction, ketoxime directing groups were shown to be necessary, but there was a very wide scope with respect to functional group compatibility on the aryl ring. Two different BCB esters were employed, as well as a BCB Weinreb amide. Finally, ethyl glyoxylate was the only electrophile employed as the second coupling partner.

Mechanistically, this reaction proceeds first by CMD, followed by insertion of the BCB internal σ-bond into the C–Rh bond (Scheme 19(b)). Next, the cyclobutyl rhodium complex **II** undergoes β-carbon elimination to give rhodacycle **III**. This species isomerises to the η^3-Rh-allyl complex **IV**, *via* a *syn*-β-hydride elimination/reinsertion sequence through a diene intermediate. Addition of the aldehyde *via* chair-like transition state **V** provides the observed stereochemistry, and protodemetalation gives the product **VI**. The authors performed several control reactions, which show that under the reaction conditions, two-component additions can occur between the C–H bond substrate and either the BCB ester (19%) or the aldehyde (68%). Nevertheless, the authors do not detect the presence of these side-products in the three-component reaction, indicating that the strain-relieving BCB insertion must outcompete direct aldehyde addition when both reactants are added.

4. Other multicomponent sequential C–H bond addition approaches

4.1. 'Reverse sequential addition' approaches

All sequential multicomponent C–H addition reactions presented thus far operate first by CMD at the C–H bond *ortho* to the directing group, followed by insertion of a π-bond or π-bond isostere, and subsequent addition to the second coupling partner. Further, each of these reactions employed either a Cp*Co(III) or Cp*Rh(III) catalyst to promote the multicomponent reaction. In 2019, Liang and co-workers reported on a new approach for multicomponent C–H addition by radical attack upon an *ortho*-metalated arene. This 'reverse sequential addition' employs a Ru(II) catalyst to enable the *meta*-functionalization of arenes (Scheme 20).[77] The authors insightfully capitalised on previously reported two-component Ru(II)-catalysed *meta*-C–H functionalization reactions and the mechanisms that had been proposed for these interesting transformations.[78–84]

In their 2019 study, Liang and co-workers coupled aryl C–H bonds with stabilised or unstabilised alkenes and fluoroalkyl halides (Scheme 20(a)). This reaction demonstrated compatibility with various directing groups, including pyridine, pyrimidine, pyrazole, and purine. The alkene scope was very broad and included styrenes, acrylates, aliphatic and internal alkenes, and dienes. Various fluoroalkyl halides as well as three examples of bromoacetates were shown to be effective coupling partners; however, more common unstabilised alkyl halides were determined to be ineffective.

In 2022, Liu and Liang expanded this reaction to enable the coupling of unstabilised alkyl halides (Scheme 20(b)).[85] To enable the coupling of these more common alkyl halides,

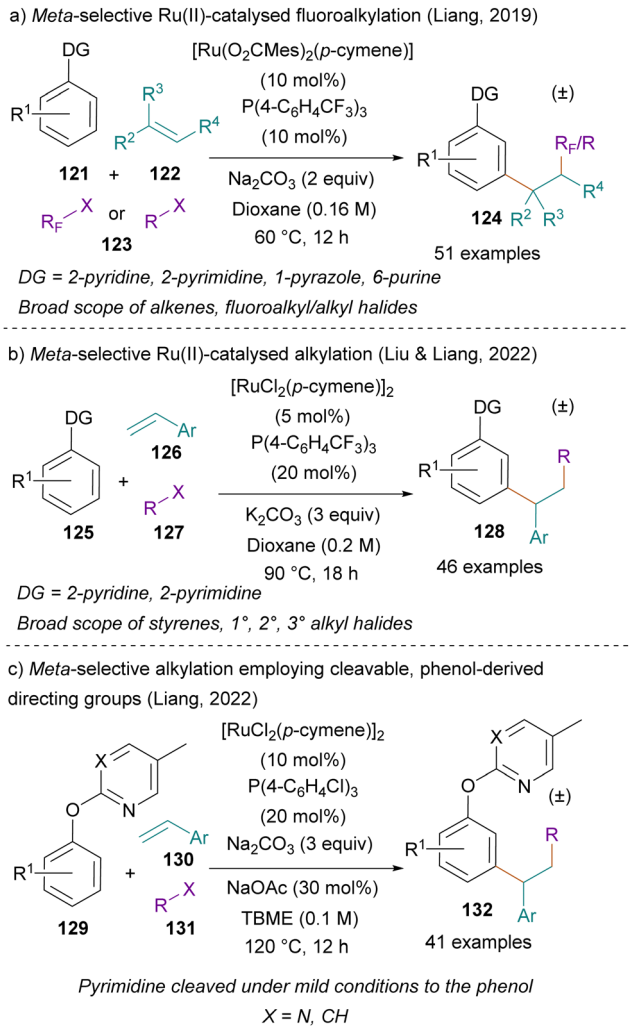

Scheme 20 *Meta*-selective, Ru-catalysed multicomponent addition operating by a reverse addition mechanism.

a slightly different Ru(II) catalyst, a different base, and a more forcing reaction temperature were used. This transformation was demonstrated for pyridine and pyrimidine directing groups, and primary, secondary, and tertiary alkyl halides were all found to be effective reactants. However, the alkene coupling partner was limited to styrenes, albeit demonstrating good scope with respect to electronics.

In the same year, Liang and co-workers further expanded the synthetic utility of this *meta*-selective transformation by employing pyrimidine- and pyridine-protected phenols as the C–H bond substrate (Scheme 20(c)).[86] These directing groups were readily cleaved to give the free phenol products, enhancing the synthetic utility of this transformation. For this reaction, increasing the temperature and using MTBE as the solvent were necessary for efficient coupling. The scope of this reaction was also limited to bromoacetates and fluoroalkyl halides, and reactivity with unstabilised alkyl halides was not reported.

The authors rigorously investigated the mechanism of these unique 'reverse sequential addition' reactions, and the proposed mechanism for the reaction in Scheme 20(a) is depicted in

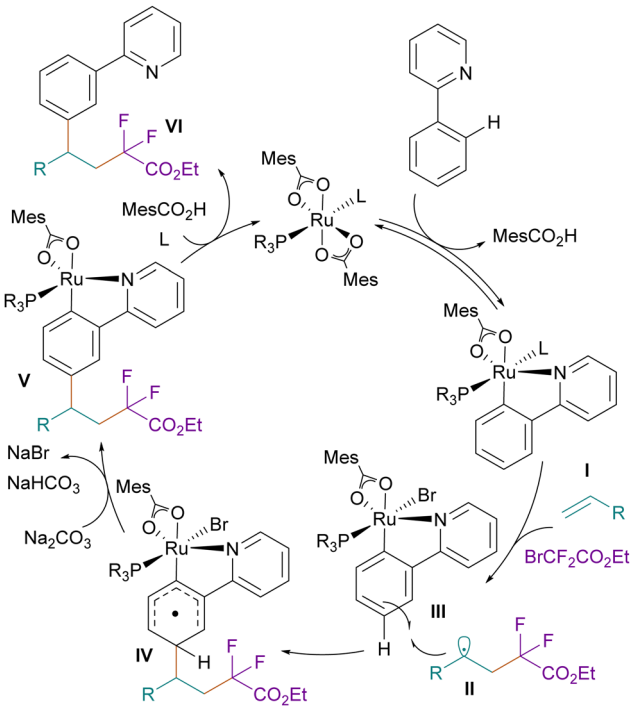

Scheme 21 Reverse addition mechanism for multicomponent alkylation.

Scheme 21.[77,85] First a CMD at the *ortho*-position of the arene C–H bond substrate resulted in ruthenacycle **I**. Next, rather than insertion of the alkene coupling partner into the C–Ru bond, ruthenacycle **I** instead undergoes a SET process with the alkyl halide. This generates an alkyl radical that regioselectively adds into the alkene coupling partner, generating the alkyl radical **II** and the Ru(III) halide **III**. The alkyl radical **II** then selectively adds into the arene *para* to the C–Ru bond, generating stabilised radical complex **IV**. The mechanism was supported by DFT studies, which showed increased Fukui indices at the position *para* to the C–Ru(III) bond, indicating enhanced susceptibility to radical attack at that position.[77,87] Ru(III) complex **IV** then rearomatises under the basic reaction conditions to give Ru(II) complex **V**, which upon protodemetalation, furnishes product **VI**. This mechanistic rationale was further supported by radical-trapping experiments with TEMPO and radical clock experiments, which indicated the presence of an alkyl radical. Additionally, deuterium labelling experiments with D_2O as the co-solvent showed no deuteration at the *meta*-positions, consistent with a reaction that does not proceed by metalation at that position.[77] Interestingly, in a separate study, Liang and co-workers showed that when 8-aminoquinoline amides were employed as directing groups rather than pyridine or pyrimidine, the radical addition occurred at the C-5 position of the aminoquinoline group instead of the cyclometalated aryl group.[88] This result underscores the potentially-tunable sensitivity of this system to electronic effects.

4.2. Other mechanistic pathways

Koenig, Chirik and co-workers reported a three-component reaction between (hetero)aryl C–H bond substrates, ethylene, and internal alkynes to furnish homoallylated arene products

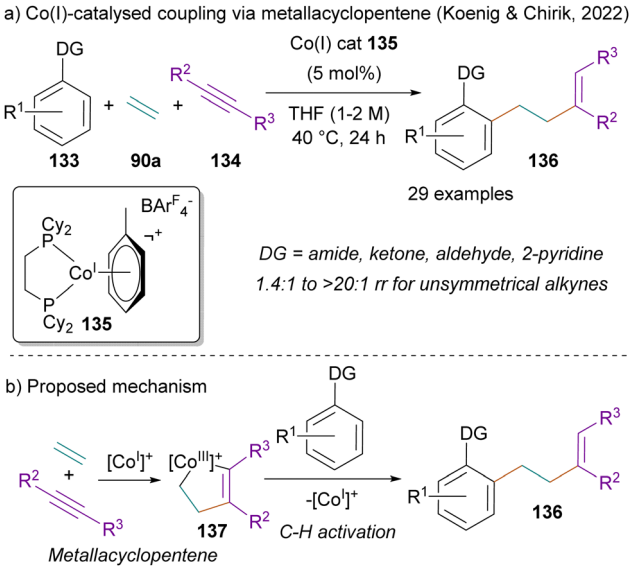

Scheme 22 Co(I)-catalysed coupling of ethylene and alkynes *via* a metallacyclopentene intermediate.

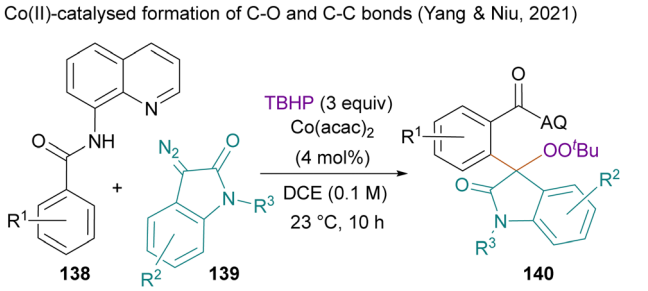

Scheme 23 Sequential addition of C–H bond to diazo compounds and a peroxide.

136 (Scheme 22(a)).[89] Employing a Co(I) pre-catalyst, the authors developed an intermolecular reaction that proceeds first *via* the formation of a Co(III) metallacyclopentene,[90,91] which subsequently undergoes C–H activation. The successful implementation of this reaction required careful catalyst design.

In aiming to form Co(III) metallacyclopentene intermediate **137** from the reaction of ethylene, alkyne, and Co(I) precatalyst **135** (Scheme 22(b)), Koenig and Chirik required a catalyst that would form a metallacyclopentene that was long-lived enough to enable intermolecular C–H activation before decomposing. Competing decomposition pathways included reductive elimination of **137** to the cyclobutene, or β-hydride elimination followed by C–H reductive elimination to furnish hydrovinylation products. After screening several alkyl bis(phosphine) ligands, the authors settled upon the strongly donating 1,2-bis-(dicyclohexylphosphino)ethane (dcpe) ligand, which was found to effectively slow the rate of the unimolecular decomposition pathways of **137**. The use of this ligand in catalyst **135** enabled a reaction that proceeds by metallacyclopentene formation followed by directed C–H activation at the *ortho*-position of the arene. Finally, reductive elimination furnishes product **136** and regenerates the Co(I) precatalyst. The mechanism was supported by multiple studies, including two-component reactions with either ethylene or 6-dodecyne. Neither produced any reactivity, pointing to the centrality of the metallacyclopentene. Deuterium labelling studies also supported the mechanism, as the use of the perdeuterated arene **133** led to deuterium incorporation at the alkenyl position of **136**, an outcome consistent with C–H activation performed by the Co(III) metallacyclopentene followed by reductive elimination.

A broad range directing groups were effective for this transformation, including primary, secondary, and tertiary amides, ketones, an aldehyde, and pyridine. The reaction was also compatible with various electronically modulating substituents at all positions on the arene. Various internal alkynes were effective coupling partners. Moreover, unsymmetrical alkynes provided products in generally good to excellent regioselectivity (1.4:1 to >20:1) with the smaller substituent placed at the R^3 position and the larger substituent at R^2 due to steric clash between the catalyst and the larger alkyne substituent during metallacycle formation.

In 2021, Yang, Niu and co-workers reported a reaction wherein a Co(II) catalyst is used to couple aryl C–H bonds with isatin-derived diazo compounds and *tert*-butyl hydroperoxide (TBHP) to form new C–C and C–O bonds (Scheme 23).[92] While the reaction is limited in scope to aminoquinoline directing groups and isatin-derived diazo compounds, this reaction expands the chemical space for such multicomponent reactions in its use of a Co(II) precatalyst. The presence of a single electron oxidant (TBHP) enables oxidation to the required Co(III) catalyst for C–H activation, suggesting that sequential C–H bond addition reactions do not need to be constrained to Cp*M(III) complexes.

5. Conclusions and outlook

Sequential C–H bond addition to two different coupling partners is a powerful new approach for the rapid, modular, and atom-economical generation of molecular complexity from simple starting inputs. A growing number of methods have been demonstrated wherein ubiquitous C–H bonds have been added across different π-systems (enones, dienes, enynes, alkynes, allenes, alkenes, and bicyclobutane alkene isosteres) and additional coupling partners (carbonyls, cyanating reagents, aminating reagents, halogenating reagents, oxygenating reagents, and alkylating reagents).

While the majority of methods described in this review employed Cp*Co(III) or Cp*Rh(III) catalysis, methods have been developed in more recent years using other metals[77,85,86] and oxidation states,[89,92] indicating that rational catalyst design may be an important avenue for further development of new sequential multicomponent C–H bond addition reactions. Due to the high modularity of this chemistry, it is likely that more combinations of existing coupling partners will be developed in a 'mix-and-match' approach. Furthermore, the chemical space of coupling partners is far from exhausted: numerous functionalities can be imagined to react in this multicomponent

approach, potentially including isocyanates, activated esters, trifluoromethylating reagents, and thiolating reagents, among many others. With the rapid expansion of research in this area, many more coupling partners are likely to be utilised, greatly increasing the numbers of products obtained by this approach.

As demonstrated in several examples,[22,33,62,73] this chemistry lends itself well to asymmetric catalysis, and with the development of new chiral ligands for group IX metal catalysed C–H functionalization,[35,65–67] additional highly enantioselective catalytic transformations can be anticipated. Furthermore, as documented in this review, the bulky chiral ligands used for asymmetric catalysis can alter product regioselectivity and diastereoselectivity relative to less sterically encumbered achiral ligands.

More generally, reactions that proceed by catalytic sequential C–H bond additions to two coupling partners often show surprising reactivity and bond connectivity and proceed by an impressive diversity of reaction mechanisms. These fascinating aspects of this research area provide great promise for the additional discovery of new reactions.

Author contributions

The original draft was prepared by D. S. B. Both authors contributed to the writing and proofreading of the manuscript.

Conflicts of interest

There are no conflicts to declare.

Acknowledgements

The NIH (R35GM122473) is acknowledged for supporting this work. D. S. B. gratefully acknowledges the Berson Graduate Research Fellowship in Chemistry for financial support.

Notes and references

1 J. Yamaguchi, A. D. Yamaguchi and K. Itami, *Angew. Chem., Int. Ed.*, 2012, **51**, 8960–9009.
2 J. Wencel-Delord and F. Glorius, *Nat. Chem.*, 2013, **5**, 369–375.
3 L. Yang and H. Huang, *Chem. Rev.*, 2015, **115**, 3468–3517.
4 T. Gensch, M. N. Hopkinson, F. Glorius and J. Wencel-Delord, *Chem. Soc. Rev.*, 2016, **45**, 2900–2936.
5 T. Cernak, K. D. Dykstra, S. Tyagarajan, P. Vachal and S. W. Krska, *Chem. Soc. Rev.*, 2016, **45**, 546–576.
6 J. R. Hummel, J. A. Boerth and J. A. Ellman, *Chem. Rev.*, 2017, **117**, 9163–9227.
7 C. Sambiagio, D. Schönbauer, R. Blieck, T. Dao-Huy, G. Pototschnig, P. Schaaf, T. Wiesinger, M. Farooq Zia, J. Wencel-Delord, T. Besset, B. U. W. Maes and M. Schnürch, *Chem. Soc. Rev.*, 2018, **47**, 6603–6743.
8 J. C. K. Chu and T. Rovis, *Angew. Chem., Int. Ed.*, 2018, **57**, 62–101.
9 P. Gandeepan, T. Müller, D. Zell, G. Cera, S. Warratz and L. Ackermann, *Chem. Rev.*, 2019, **119**, 2192–2452.
10 L. Lukasevics, A. Cizikovs and L. Grigorjeva, *Chem. Commun.*, 2021, **57**, 10827–10841.
11 T. Satoh and M. Miura, *Chem. – Eur. J.*, 2010, **16**, 11212–11222.
12 G. Song, F. Wang and X. Li, *Chem. Soc. Rev.*, 2012, **41**, 3651–3678.
13 J. A. Boerth and J. A. Ellman, *Chem. Sci.*, 2016, **7**, 1474–1479.
14 Y. Fukui, P. Liu, Q. Liu, Z.-T. He, N.-Y. Wu, P. Tian and G.-Q. Lin, *J. Am. Chem. Soc.*, 2014, **136**, 15607–15614.
15 T. Piou and T. Rovis, *Nature*, 2015, **527**, 86–90.
16 A. Lerchen, T. Knecht, C. G. Daniliuc and F. Glorius, *Angew. Chem., Int. Ed.*, 2016, **55**, 15166–15170.
17 H. Li, Y. Li, X.-S. Zhang, K. Chen, X. Wang and Z.-J. Shi, *J. Am. Chem. Soc.*, 2011, **133**, 15244–15247.
18 M. Tang, Y. Li, S. Han, L. Liu, L. Ackermann and J. Li, *Eur. J. Org. Chem.*, 2019, 660–664.
19 J. A. Boerth, J. R. Hummel and J. A. Ellman, *Angew. Chem., Int. Ed.*, 2016, **55**, 12650–12654.
20 J. R. Hummel and J. A. Ellman, *J. Am. Chem. Soc.*, 2015, **137**, 490–498.
21 M. T. Robak, M. A. Herbage and J. A. Ellman, *Chem. Rev.*, 2010, **110**, 3600–3740.
22 A. G. Herraiz and N. Cramer, *ACS Catal.*, 2021, **11**, 11938–11944.
23 S.-S. Zhang, J. Xia, J.-Q. Wu, X.-G. Liu, C.-J. Zhou, E. Lin, Q. Li, S.-L. Huang and H. Wang, *Org. Lett.*, 2017, **19**, 5868–5871.
24 J. A. Boerth, S. Maity, S. K. Williams, B. Q. Mercado and J. A. Ellman, *Nat. Catal.*, 2018, **1**, 673–679.
25 R. Li, C.-W. Ju and D. Zhao, *Chem. Commun.*, 2019, **55**, 695–698.
26 Z. Shen, C. Li, B. Q. Mercado and J. A. Ellman, *Synthesis*, 2020, 1239–1246.
27 S. Dongbang, Z. Shen and J. A. Ellman, *Angew. Chem., Int. Ed.*, 2019, **58**, 12590–12594.
28 I. Marek and G. Sklute, *Chem. Commun.*, 2007, 1683–1691.
29 I. Marek, Y. Minko, M. Pasco, T. Mejuch, N. Gilboa, H. Chechik and J. P. Das, *J. Am. Chem. Soc.*, 2014, **136**, 2682–2694.
30 K. W. Quasdorf and L. E. Overman, *Nature*, 2014, **516**, 181–191.
31 J. Yang, D.-W. Ji, Y.-C. Hu, X.-T. Min, X. Zhou and Q.-A. Chen, *Chem. Sci.*, 2019, **10**, 9560–9564.
32 T. Pinkert, T. Wegner, S. Mondal and F. Glorius, *Angew. Chem., Int. Ed.*, 2019, **58**, 15041–15045.
33 R. Mi, X. Zhang, J. Wang, H. Chen, Y. Lan, F. Wang and X. Li, *ACS Catal.*, 2021, **11**, 6692–6697.
34 S. Y. Hong, Y. Hwang, M. Lee and S. Chang, *Acc. Chem. Res.*, 2021, **54**, 2683–2700.
35 C. G. Newton, D. Kossler and N. Cramer, *J. Am. Chem. Soc.*, 2016, **138**, 3935–3941.
36 S. Dongbang and J. A. Ellman, *Angew. Chem., Int. Ed.*, 2021, **60**, 2135–2139.
37 F. F. Fleming, L. Yao, P. C. Ravikumar, L. Funk and B. C. Shook, *J. Med. Chem.*, 2010, **53**, 7902–7917.

38 M. Gehringer and S. A. Laufer, *J. Med. Chem.*, 2019, **62**, 5673–5724.
39 V. Y. Kukushkin and A. J. L. Pombeiro, *Chem. Rev.*, 2002, **102**, 1771–1802.
40 G. Dilauro, M. Dell'Aera, P. Vitale, V. Capriati and F. M. Perna, *Angew. Chem., Int. Ed.*, 2017, **56**, 10200–10203.
41 M. S. M. Pearson-Long, F. Boeda and P. Bertus, *Adv. Synth. Catal.*, 2017, **359**, 179–201.
42 Y. Ping, Q. Ding and Y. Peng, *ACS Catal.*, 2016, **6**, 5989–6005.
43 M. Chaitanya and P. Anbarasan, *Org. Biomol. Chem.*, 2018, **16**, 7084–7103.
44 A. B. Pawar and S. Chang, *Org. Lett.*, 2015, **17**, 660–663.
45 H. Wang, I. Choi, T. Rogge, N. Kaplaneris and L. Ackermann, *Nat. Catal.*, 2018, **1**, 993–1001.
46 L. V. Myznikov, A. Hrabalek and G. I. Koldobskii, *Chem. Heterocycl. Compd.*, 2007, **43**, 1–9.
47 C. Xu, J. P. Tassone, B. Q. Mercado and J. A. Ellman, *Angew. Chem., Int. Ed.*, 2022, e202202364.
48 J. Le Bras and J. Muzart, *Chem. Soc. Rev.*, 2014, **43**, 3003–3040.
49 B. Alcaide and P. Almendros, *Acc. Chem. Res.*, 2014, **47**, 939–952.
50 J. M. Alonso and P. Almendros, *Chem. Rev.*, 2021, **121**, 4193–4252.
51 J. A. Boerth and J. A. Ellman, *Angew. Chem., Int. Ed.*, 2017, **56**, 9976–9980.
52 K. C. Nicolaou, P. G. Bulger and D. Sarlah, *Angew. Chem., Int. Ed.*, 2005, **44**, 4442–4489.
53 G. Evano, N. Blanchard and M. Toumi, *Chem. Rev.*, 2008, **108**, 3054–3131.
54 R. Jana, T. P. Pathak and M. S. Sigman, *Chem. Rev.*, 2011, **111**, 1417–1492.
55 D.-G. Yu, T. Gensch, F. de Azambuja, S. Vásquez-Céspedes and F. Glorius, *J. Am. Chem. Soc.*, 2014, **136**, 17722–17725.
56 H. Ikemoto, T. Yoshino, K. Sakata, S. Matsunaga and M. Kanai, *J. Am. Chem. Soc.*, 2014, **136**, 5424–5431.
57 R. Tanaka, H. Ikemoto, M. Kanai, T. Yoshino and S. Matsunaga, *Org. Lett.*, 2016, **18**, 5732–5735.
58 S. Wang, J.-T. Hou, M.-L. Feng, X.-Z. Zhang, S.-Y. Chen and X.-Q. Yu, *Chem. Commun.*, 2016, **52**, 2709–2712.
59 C. Grohmann, H. Wang and F. Glorius, *Org. Lett.*, 2013, **15**, 3014–3017.
60 P. Patel and S. Chang, *Org. Lett.*, 2014, **16**, 3328–3331.
61 Y. Park, Y. Kim and S. Chang, *Chem. Rev.*, 2017, **117**, 9247–9301.
62 S. Maity, T. J. Potter and J. A. Ellman, *Nat. Catal.*, 2019, **2**, 756–762.
63 T. C. Nugent, *Chiral Amine Synthesis: Methods, Developments and Applications*, Wiley-VCH GmbH & Co., Weinheim, Germany, 2010.
64 B. Ye and N. Cramer, *J. Am. Chem. Soc.*, 2013, **135**, 636–639.
65 C. G. Newton, S.-G. Wang, C. C. Oliveira and N. Cramer, *Chem. Rev.*, 2017, **117**, 8908–8976.
66 T. Yoshino, S. Satake and S. Matsunaga, *Chem. – Eur. J.*, 2020, **26**, 7346–7357.
67 J. Mas-Roselló, A. G. Herraiz, B. Audic, A. Laverny and N. Cramer, *Angew. Chem., Int. Ed.*, 2021, **60**, 13198–13224.
68 F. W. Patureau, J. Wencel-Delord and F. Glorius, *Aldrichimica Acta*, 2012, **45**, 31–41.
69 H. Lei and T. Rovis, *J. Am. Chem. Soc.*, 2019, **141**, 2268–2273.
70 T. Knecht, S. Mondal, J.-H. Ye, M. Das and F. Glorius, *Angew. Chem., Int. Ed.*, 2019, **58**, 7117–7121.
71 J. S. Burman, R. J. Harris, C. M. B. Farr, J. Bacsa and S. B. Blakey, *ACS Catal.*, 2019, **9**, 5474–5479.
72 D. S. Brandes, A. D. Muma and J. A. Ellman, *Org. Lett.*, 2021, **23**, 9597–9601.
73 D. S. Brandes, A. Sirvent, B. Q. Mercado and J. A. Ellman, *Org. Lett.*, 2021, **23**, 2836–2840.
74 N. Koga, S. Obara, K. Kitaura and K. Morokuma, *J. Am. Chem. Soc.*, 1985, **107**, 7109–7116.
75 S. V. Kumar, A. Yen, M. Lautens and P. J. Guiry, *Chem. Soc. Rev.*, 2021, **50**, 3013–3093.
76 T. Pinkert, M. Das, M. L. Schrader and F. Glorius, *J. Am. Chem. Soc.*, 2021, **143**, 7648–7654.
77 X.-G. Wang, Y. Li, H.-C. Liu, B.-S. Zhang, X.-Y. Gou, Q. Wang, J.-W. Ma and Y.-M. Liang, *J. Am. Chem. Soc.*, 2019, **141**, 13914–13922.
78 N. Hofmann and L. Ackermann, *J. Am. Chem. Soc.*, 2013, **135**, 5877–5884.
79 A. J. Paterson, S. John-Campbell, M. F. Mahon, N. J. Press and C. G. Frost, *Chem. Commun.*, 2015, **51**, 12807–12810.
80 J. Li, S. Warratz, D. Zell, S. De Sakar, E. E. Ishikawa and L. Ackermann, *J. Am. Chem. Soc.*, 2015, **137**, 13894–13901.
81 C. J. Teskey, A. Y. W. Lui and M. F. Greaney, *Angew. Chem., Int. Ed.*, 2015, **54**, 11677–11680.
82 Q. Yu, L. Hu, Y. Wang, S. Zheng and J. Huang, *Angew. Chem., Int. Ed.*, 2015, **54**, 15284–15288.
83 Z. Fan, J. Ni and A. Zhang, *J. Am. Chem. Soc.*, 2016, **138**, 8470–8475.
84 M. T. Mihai, G. R. Genov and R. J. Phipps, *Chem. Soc. Rev.*, 2018, **47**, 149–171.
85 H.-C. Liu, X.-P. Gong, Y.-Z. Wang, Z.-J. Niu, H. Yue, X.-Y. Liu and Y.-M. Liang, *Org. Lett.*, 2022, **24**, 3043–3047.
86 Y.-Y. Luan, X.-Y. Gou, W.-Y. Shi, H.-C. Liu, X. Chen and Y.-M. Liang, *Org. Lett.*, 2022, **24**, 1136–1140.
87 K. Korvorapun, N. Kaplaneris, T. Rogge, S. Warratz, A. C. Stückl and L. Ackermann, *ACS Catal.*, 2018, **8**, 886–892.
88 W.-Y. Shi, Y.-N. Ding, C. Liu, N. Zheng, X.-Y. Gou, M. Li, Z. Zhang, H.-C. Liu, Z.-J. Niu and Y.-M. Liang, *Chem. Commun.*, 2020, **56**, 12729–12732.
89 W. G. Whitehurst, J. Kim, S. G. Koenig and P. J. Chirik, *J. Am. Chem. Soc.*, 2022, **144**, 4530–4540.
90 W. Ma, C. Yu, T. Chen, L. Xu, W.-X. Zhang and Z. Xi, *Chem. Soc. Rev.*, 2017, **46**, 1160–1192.
91 A. Roglans, A. Pla-Quintana and M. Solà, *Chem. Rev.*, 2021, **121**, 1894–1979.
92 M.-H. Li, X.-J. Si, H. Zhang, D. Yang, J.-L. Niu and M.-P. Song, *Org. Lett.*, 2021, **23**, 914–919.

